Indian Geotech J (March 2017) 47(1):2–34
DOI 10.1007/s40098-016-0215-5

ORIGINAL PAPER

The Geosynthetics for Sustainable Construction of Infrastructure Projects

Rajagopal Karpurapu[1]

Received: 1 December 2016 / Accepted: 6 December 2016 / Published online: 29 December 2016

Abstract The introduction of geosynthetics has drastically changed the manner of geotechnical practice. The challenges posed by the uncertainty of soil properties are easily overcome by the intelligent use of geosynthetics. The geosynthetics are applied practically in all areas of geotechnical engineering including the construction of steep slopes, retaining walls, ground improvement systems, landfills, drainage and filtration control around geotechnical structures, erosion control, etc. This lecture will briefly describe the history of geosynthetics and their applications to different infrastructure construction projects. The aspects of environmental sustainability that can be achieved through the use of geosynthetics are briefly brought out towards the end of the lecture.

Keywords Geosynthetics · Infrastructure projects · Soil retaining walls · Steep embankments · Landfills · Sustainability · Vacuum consolidation · Geosynthetic load transfer platform

List of symbols

σ_3, σ_1	Minor and major principal stresses
σ_{1u}, σ_{1R}	Major principal stresses in unreinforced and reinforced soil samples
K_a	Rankine's active earth pressure coefficient
K_p	Rankine's passive earth pressure coefficient
$\bar{c}$	Apparent cohesive strength of soil
ϕ	Friction angle of soil
ϕ_u, ϕ_R	Friction angles of unreinforced and reinforced soils
$\Delta\sigma_1$	Increase in major principal stress
S_v, S_h	Vertical and horizontal spacing of reinforcement layers
P	Force in the reinforcement layer
σ_v	Normal pressure on the interface
α	Angle between horizontal and reinforcement layer
ε_a	Axial strain
ε_c	Circumferential strain
M	secant modulus of geosynthetic
p	Mean normal stress = $(\sigma_1 + \sigma_3)/2$
q	Shear stress = $(\sigma_1 - \sigma_3)/2$
H	Height of embankment
a	Diameter of pile
$\bar{x}$	Depth of neutral plane below ground surface
ℓ_{crit}	Critical length of the floating pile
C_c	Arching coefficient
FS	Factor of safety against slip circle failure
ESC	Encased stone column
OSC	Ordinary stone column

Introduction

Ever since Karl Terzaghi had initiated the field of Soil Mechanics (geotechnical engineering for the new age generation) with his classical book [1], the field of geotechnical engineering has evolved over the years. The concepts have evolved with the engineers gaining experience with each completed project, and most importantly the failures! Karl Terzaghi has himself developed and re-

✉ Rajagopal Karpurapu
gopalkr@iitm.ac.in

[1] Department of Civil Engineering, Indian Institute of Technology Madras, Chennai, TN 600 036, India

developed (calibrated) several of his theories on bearing capacity, drainage and filtration, deep excavations, etc. over a period of time.

The soil being a natural material, its properties and availability of suitable variety are mostly uncertain. This poses major challenge to geotechnical engineers. To make the things even more complicated, all soil structures are exposed to natural elements like wind and rain induced erosion, floods and earthquakes. The success of geotechnical engineering profession is best described by the saying "Failure is the stepping stone to success". Each geotechnical failure is followed by deep rethink on the possible reasons for the failure, leading to further improvements in the geotechnical practice. Some of these failures can be attributed to the use of inappropriate type of soil, poor quality of soil compaction. Most importantly, the significant reason for geotechnical failures could be attributed to the uncertainty and large variability in the soil properties. For example, the designs for filtration and drainage, etc. are the most difficult to implement in the field due to the requirement for particular size of particles arranged in layers. Hence, it is necessary to utilize other techniques to improve the soil properties or introduce other materials into the soil to improve its behaviour. The modern geosynthetics address the issue of helping the poor quality soil to cope up with the engineering demands.

The introduction of geosynthetics probably has the most impact on the way geotechnical engineering is practiced today. The geosynthetics have potential applications in all areas of geotechnical engineering. As these products are factory produced, they have fairly well known properties which can be used to address several issues faced by geotechnical engineers including erosion, filtration, drainage, stabilization, etc.

Well before the coining of the words *geotextile* or *geosynthetic*, ancient humans had understood the advantages of using soil composites for construction purposes. For example, in ancient Mesopotamia, (present day Iraq and parts of Iran, Syria and Turkey), Babylonians had built 30–40 m high towers (Ziggurats) for religious purposes using soil reinforced with tree branches, leaves, ropes, etc. Parts of the Great Wall of China were reinforced with leaves, tree trunks and branches. The Adobe bricks in North Africa and South America were made by using straw to improve the quality of bricks. In rural areas of India, placing of bamboo mats inside the mud walls of the dwellings is quite common. Similar bamboo mats and mats made of coconut leaves are used for construction over soft clay soils in Kerala. In North-East parts of India, it is common to build bridges across rivers using plant roots (https://en.wikipedia.org/wiki/Living_root_bridges).

The family of geosynthetics consists of a wide array of products including geotextiles, geogrids, geomembranes, geonets, pre-fabricated vertical drains, asphalt overlay fabrics, geomats, geocells, drain boards, geo-composites which consist of one or more different products for multiple functions [2]. The variety of new geosynthetic products is ever increasing. The latest products in this family are the electro-kinetic geosynthetics which combine the electrical conductivity and reinforcement properties for enabling the use of marginal soils in reinforced soil structures. This technique can be used for dewatering, accelerated consolidation, quick drainage, strengthening of marginal soils, slope stabilization, etc. (www.electrokinetic.co.uk).

Brief History of Geosynthetics

Before the word *geosynthetics* was coined, all related products were lumped under the banner, *geotextiles*. Way back in the year 1986, Giroud has described the progression in this field with his land mark lecture titled "From Geotextiles to Geosynthetics: A Revolution in Geotechnical Engineering" at the 3rd International Conference on Geotextiles in Vienna [3]. In the lecture, he had commented that "it is no longer possible to do geotechnical engineering without geotextiles". This statement is more valid in the year 2016 with several new and innovative geosynthetic products. Some examples for this are the use of geosynthetic pre-fabricated vertical drains (PVDs) for accelerated consolidation of soils in place of sand drains, reinforced soil walls in place of reinforced concrete walls, steep reinforced soil slopes in place of shallow unreinforced slopes, geosynthetic composite drains in place of thick layers of stone aggregate, etc.

Some major milestones in the development of polymer technology can be chronicled as follows:

- 1913—PVC (polyvinyl chloride) was developed
- 1930—nylon (polyamide fibre) was developed
- 1941—polyester fibre was developed
- 1949—polyethylene filaments were developed
- 1954—polypropylene fibres were developed
- 1960's—technology for manufacture of nonwoven fabrics was developed
- 1967—Development of synthetic nets by Netlon UK for soil reinforcement applications

Some early applications in this field are:

- Use of corduroy mats for pavements in South Carolina, USA during 1920's and 1930's
- Use of canvas sheets for ease of army vehicle movement during the 2nd World war
- Use of sand bags made of nylon woven fabrics (Nicolon) in Netherlands in 1957

- Use of woven fabrics between rip-rap and soil in Florida for coastal erosion protection in 1958
- Use of synthetic sand bags for canal lining in West Germany in 1958
- Use of synthetic sand bags for coastal erosion protection in Japan in 1958–1959 period
- Use of sand filled nylon mattresses for coastal erosion protection in the Netherlands in 1960
- Use of nonwoven fabric as asphalt overlay in USA in the year 1966

The use of geomembranes for canal and landfill lining dates back to 1960's in US and Europe. Henri Vidal had applied for patent for the reinforced soil (*Terre Armee*) in the year 1963. The construction of reinforced soil retaining walls and embankments started from late 1960's and early 1970's with the Reinforced Earth technology. With the introduction of the stretched geogrid products by Netlon UK, the use of polymeric reinforcement layers in reinforced soil retaining walls and embankments picked up from early 1980's.

The first International Conference on geosynthetics titled "International Conference on the use of fabrics in geomechanics" was held at Paris in the year 1977. The International Geotextile Society (IGS) was formed in the year 1983. Later its name was changed to International Geosynthetics Society to reflect the fact that the geosynthetics encompass the entire family of related products (viz. Geotextiles, geogrids, geomembranes, geonets, etc.) in the year 1994. More details of the history of IGS can be found at www.geosyntheticssociety.org.

Brief history of Geosynthetic Applications in India

Excellent summary on the development and applications of geosynthetic technology in India can be found in [4–6]. First workshop on geotextiles was held at New Delhi in the year 1985. The story of the geosynthetics development in India is reported by Rao et al. [7].

The geosynthetic related activity in India started from the middle of 1980's with the construction of road over rail bridge at Ludhiana in 1985 using polymeric reinforcement strips and pond ash as the backfill material. The height of the structure was about 8 m. A cost saving of 15% was reported for this wall along with savings in construction time due to the expedient nature of this technique. More details of different geosynthetic structures can be found in [6, 7]. Particular contribution of India to geosynthetics is on the natural geosynthetic materials made of coir and jute. These products are used in several geosynthetic applications such as erosion control, drainage and filtration, construction of low volume roads, accelerated consolidation, paver fabric to control reflection cracking in flexible pavements, etc. The different functions that can be achieved using geosynthetics include reinforcement, separation, drainage, filtration, fluid barrier, erosion control [2].

Strength Theories of Reinforced Soil

The strength of the reinforced soil is the most important parameter for all design applications of structures like retaining walls and reinforced soil embankments. The reinforced soil is a composite material consisting of soil and reinforcement. The soil is strong in compression and the reinforcement is strong in tension. The synergetic combination of soil and reinforcement produces an excellent material that can be used for construction purposes. These reinforcement materials are made of polymeric, metallic or natural materials and placed in the soil as horizontal layers. In some systems, the reinforcement is introduced into the soil as short length discrete fibres [8]. While the geosynthetic reinforcement layers are planar, the three-dimensional form of geosynthetics, geocells, provide excellent all round confinement to the soil even at low normal pressures leading to improved performance of the soil [9, 10].

The strength of the reinforced soil can be studied either using triaxial compression tests or direct shear tests. Figure 1 shows the stress–strain response of dry granular soil tested in a triaxial compression apparatus at 25 kPa confining pressure and different number of horizontal reinforcement layers (50 mm diameter and 100 mm height) [11].

It could be seen that as the number of reinforcement layers is increased, the strength and modulus of the soil increases. The contribution of the reinforcement layers is dependent on the number of reinforcement layers, strength, stiffness and confining pressure. As the confining pressure is increased, the inherent strength of the soil increases and

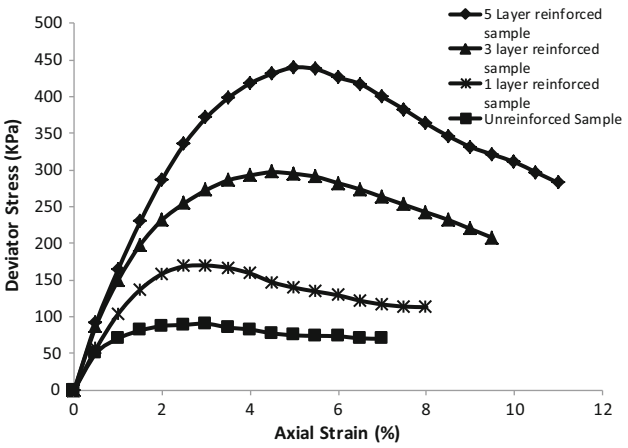

Fig. 1 Stress–strain response of dry granular soil at 25 kPa confining pressure

the influence of the reinforcement is significantly reduced. This result is illustrated in Fig. 2, where the strength of unreinforced soil is compared with that of 5 reinforcement layers and 200 kPa confining pressure. From the results in Figs. 1 and 2, it could be observed that the relative increase at higher confining pressures is lesser compared to that at lower confining pressures for the same number of reinforcement layers. From the data in the same figures, it could also be observed that the influence of reinforcement layers on the modulus of the reinforced soil is larger at lower confining pressures compared to that at higher confining pressure. The slope of the stress–strain curves at lower confining pressures increased rapidly at lower confining pressure (Fig. 1) while the slope remained the same until large strain levels at higher confining pressure (Fig. 2). Similar observations were also reported by Chandrasekaran et al. [12].

The strength properties of the reinforced soil can be easily understood from the conventional Mohr circle diagrams and the Mohr–Coulomb strength theory in terms of cohesion (c) and friction angle (ϕ). The strength of the reinforced soil can be interpreted in terms of increase in friction angle or apparent cohesion or increase in confining pressure as illustrated in the following [13, 14]. The reinforced soil tested at the same confining pressure as the corresponding unreinforced soil will develop higher limit stress as illustrated in Fig. 3. The friction angles of unreinforced and reinforced soils can be interpreted from the corresponding Mohr circles and Mohr strength envelopes. The same strength increase can be interpreted in terms of apparent cohesion as illustrated in Fig. 4.

The strength of the dry granular unreinforced soil can be written as,

$$\sigma_{1u} = \sigma_3 K_p \tag{1}$$

in the above, σ_{1u} is the limiting vertical stress while σ_3 is the corresponding confining pressure and K_p is the passive

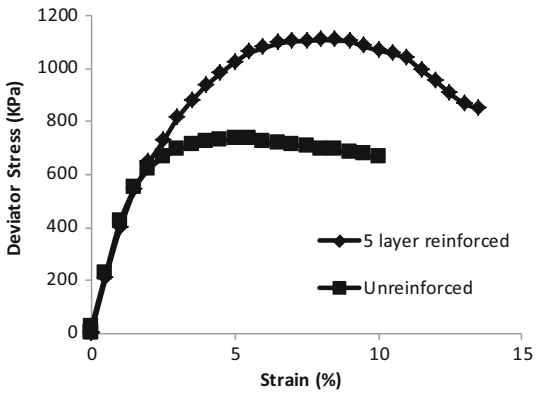

Fig. 2 Stress–strain response of dry granular soil at 200 kPa confining pressure

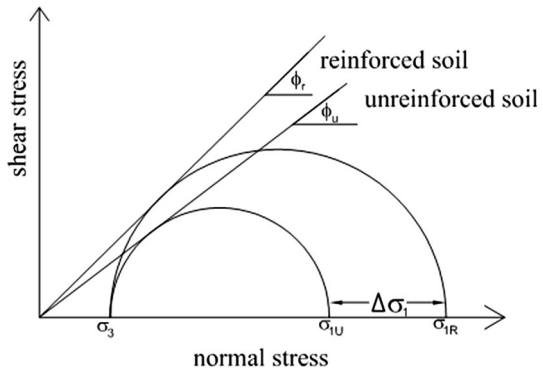

Fig. 3 Increase in friction angle of dry granular soil with reinforcement layers

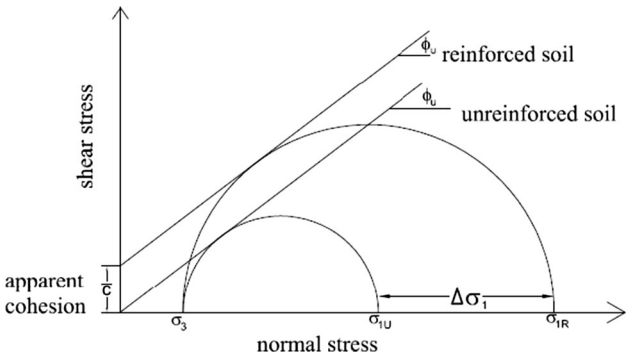

Fig. 4 Apparent cohesion in reinforced soil

earth pressure coefficient written as $(1 + \sin\phi)/(1 - \sin\phi)$ in terms of the friction angle of the soil. When the soil with reinforcement layers is tested, the strength increases to σ_{1R}. The slope of the strength envelope of reinforced soil can be fixed as the same as that of unreinforced soil (frictional strength is assumed to remain the same) and the increase in shear strength can be attributed to the development of apparent cohesion. Hence, the increased strength of the reinforced soil can be expressed in terms of the apparent cohesion as follows,

$$\sigma_{1R} = \sigma_3 K_p + 2 \cdot \bar{c} \cdot \sqrt{K_p} \tag{2}$$

in which σ_{1R} is the limiting strength of the reinforced soil and $\bar{c}$ is the apparent cohesion developed in the reinforced soil.

From Eqs. 1 and 2, the apparent cohesion induced in the soil due to the reinforcement layers can be written as,

$$\bar{c} = \frac{\sigma_{1R} - \sigma_{1u}}{2\sqrt{K_p}} = \frac{\Delta\sigma_1}{2\sqrt{K_p}} \tag{3}$$

The strength increase of reinforced soil can also be interpreted in terms of an increase in confining pressure as illustrated in Fig. 5. The strength of the reinforced soil can be written as,

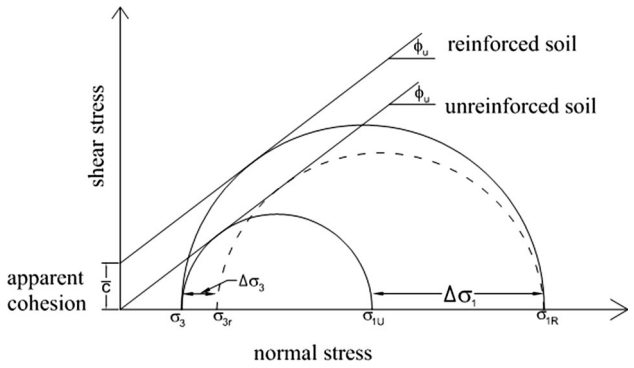

Fig. 5 Increase in confining pressure in reinforced soil

$$\sigma_{1R} = (\sigma_3 + \Delta\sigma_3)K_p = \sigma_3 K_p + 2 \cdot \bar{c} \cdot \sqrt{K_p}$$
$$\Rightarrow \Delta\sigma_3 = \frac{2\bar{c}}{\sqrt{K_p}} \tag{4}$$

In all these above equations, the confining pressure ($\Delta\sigma_3$) developed due to the placement of reinforcement layers due to a reinforcement force of P, can be written as,

$$\Delta\sigma_3 = \frac{P}{S_v \cdot S_h} \tag{5}$$

in which S_v and S_h are the vertical and horizontal spacings of the reinforcement layers. The force P is computed as the lower of the rupture strength of the reinforcement or the pullout capacity. The rupture capacity of geosynthetic reinforcement is estimated based on its index tensile strength and different long term factors like creep reduction, construction induced damage, chemical and biological degradation factors, importance factor, etc. The pullout capacity is estimated based on the embedment length (L), normal pressure on the interface (σ_v), interface friction angle (δ), width of reinforcement layer (B) as,

$$R_p = 2 \times \sigma_v \times \tan\delta \times L \times B \tag{6}$$

Hausmann [15] has given a slightly different interpretation for the strength of reinforced soil. He proposed that the reinforced soil can be tested at a lower confining pressure to develop the same limiting strength as that of the unreinforced soil as illustrated in Fig. 6.

$$\sigma_{3u} = K_A \sigma_1$$
$$K_A = \frac{1 - \sin\phi_u}{1 + \sin\phi_u}$$
$$\sin\phi_u = \frac{\sigma_1 - \sigma_{3u}}{\sigma_1 + \sigma_{3u}}$$
$$\sin\phi_r = \frac{\sigma_1 - \sigma_{3r}}{\sigma_1 + \sigma_{3r}} = \frac{\sigma_1 - (\sigma_{3u} - \Delta\sigma_3)}{\sigma_1 + (\sigma_{3r} - \Delta\sigma_3)} = \frac{1 - \frac{\sigma_{3u}}{\sigma_1} + \frac{\Delta\sigma_3}{\sigma_1}}{1 + \frac{\sigma_{3u}}{\sigma_1} - \frac{\Delta\sigma_3}{\sigma_1}}$$
$$= \frac{1 - K_A + F}{1 + K_A - F} \tag{7}$$

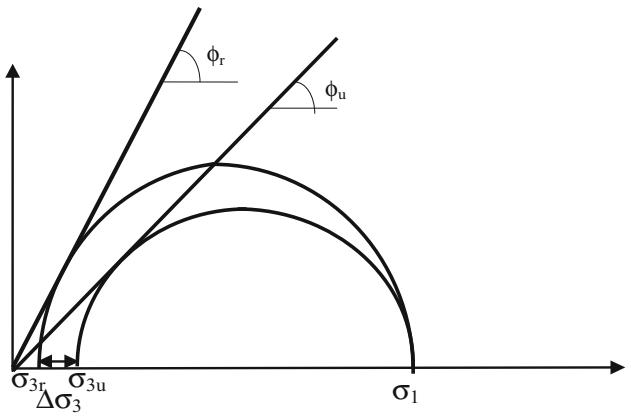

Fig. 6 Mohr *circles* for reinforced and unreinforced soils developing the same limiting stress

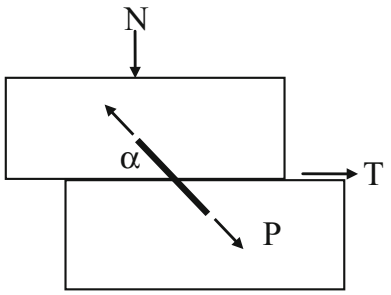

Fig. 7 Schematic of direct shear test on reinforced soil

The factor F depends on the additional confining pressure developed due to the placement of reinforcement layers in the soil.

The interpretation for the strength of the reinforced soil in direct shear tests can be performed in terms of the increase in normal and shear stresses due to the force developed in the reinforcement layer. The Fig. 7 illustrates the behaviour of a reinforced soil under direct shear.

The relation between the normal force N and the limiting shear force T for the unreinforced soil can be written as,

$$T = N \cdot \tan\phi \tag{8}$$

If the tensile force developed in the reinforcement layer is P, the limiting shear force for the reinforced soil can be written as follows including the vertical and horizontal components of the reinforcement force [16],

$$T_r = (N + P\ \sin\alpha) \cdot \tan\phi + P \cdot \cos\alpha \tag{9}$$

From the above, the strength increase due to reinforcement layers in the direct shear mode can be understood. Similar mechanism can be extended to understand the influence of reinforcement layers on the strength of reinforced soil slopes.

Sandwich Technique to Improve Performance of Reinforced Soil

The strength of the reinforced soil is very much a function of the friction angle of the soil. It is best to use well graded granular soil as backfill that can mobilize large friction angles and thereby improve the interaction between the reinforcement layers and the soil. In fact, all the design codes like BS 8006 [17], FHWA [18] recommend the use of granular soil backfill with high friction angles. In case, the backfill soil is of poor quality with low strength, the strength of the reinforced soil can be increased by sandwiching the reinforcement layers in thin layers of stronger granular soils [19–21]. The necessity of the strong soil in the sandwich layers around the reinforcement is due to the higher shear stresses around the reinforcement compared to the body of the soil as reported by Milligan et al. [22]. If stronger soil is placed around the reinforcement layer, the soil–reinforcement interface does not undergo premature failure leading to better load transfer from soil to the reinforcement.

The above is illustrated through the results from triaxial compression tests performed on a clay soil reinforced with a soft mesh and different thicknesses of sand layers, Fig. 8 (100 mm diameter and 200 mm height). The required thickness of the granular layers around the reinforcement layers were obtained by carefully placing pre-weighed quantities of granular soil around the reinforcement. It is clear from this result that the sandwich technique can be used to improve the strength of reinforced soil with poor backfill soils. In addition to the improvement in the strength, the sand layers can also function as drainage layers to dissipate the excess pore pressures [21]. The performance of the same soil under repeated loading is shown in Fig. 9 in terms of the axial strain developed at the end of different number of cycles. It is clearly seen that with the placement of sandwich layers, the reinforced soil sample requires much larger number of cycles of loading to develop the same strain levels as in the plain reinforced and unreinforced soil samples. This result clearly shows the advantage of the thin sand layers placed around the reinforcement that enables better interaction between the reinforcement layer and the backfill soil leading to higher strength of the reinforced soil.

In order to understand the effect of the sandwich layers on the performance of reinforced soil embankments under repeated loading, finite element analyses were performed on a 3 m high embankment as shown in Fig. 10. The performance of the embankment under repeated loading applied on the surface was examined in [20] using the finite element code GEOFEM2D, [23] and hierarchical

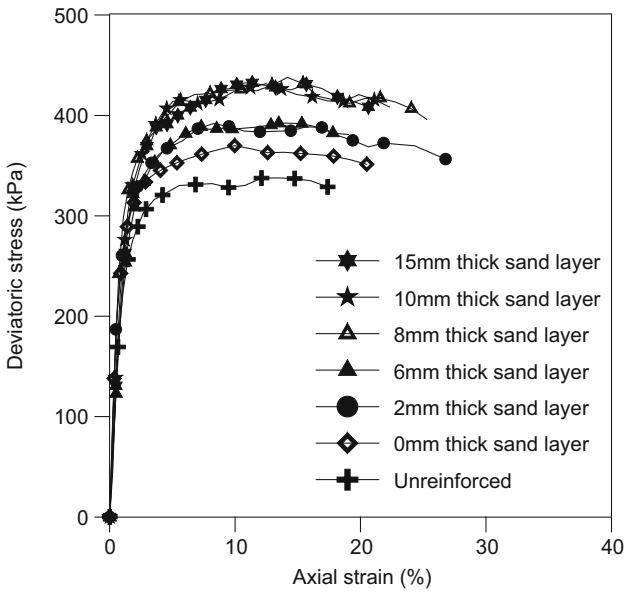

Fig. 8 Stress–strain behaviour of reinforced clay soil ($\sigma_3 = 100$ kPa) [20]

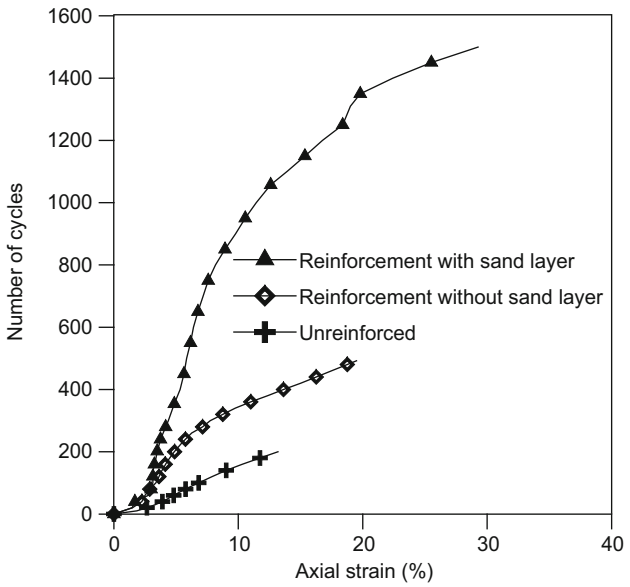

Fig. 9 Axial strain development under repeated loading ($\sigma_3 = 100$ kPa) [20]

constitutive model developed by Wathugala and Desai [24]. The normalized horizontal deformations at the toe with and without sandwich layers are compared in Fig. 11. The displacements have reached a steady state response within the first few cycles for the sandwich case while the displacements continued to increase without the sandwich layers. This result once again demonstrates the advantage of providing thin layers of granular soil around the reinforcement.

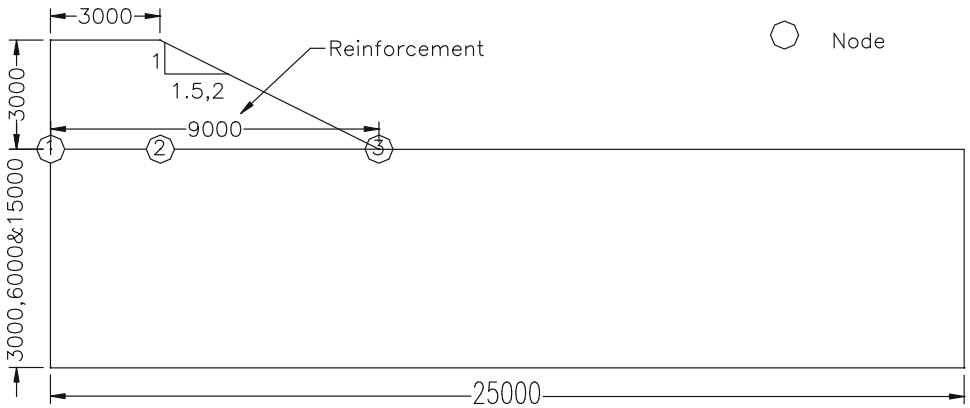

Fig. 10 3 m high embankment resting on soft clay soil with a basal reinforcement layer [20]

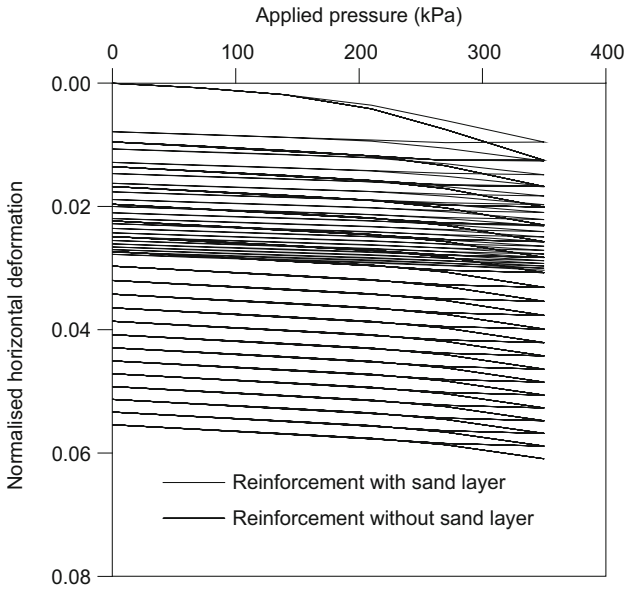

Fig. 11 Accumulation of permanent deformations under repeated loading [20]

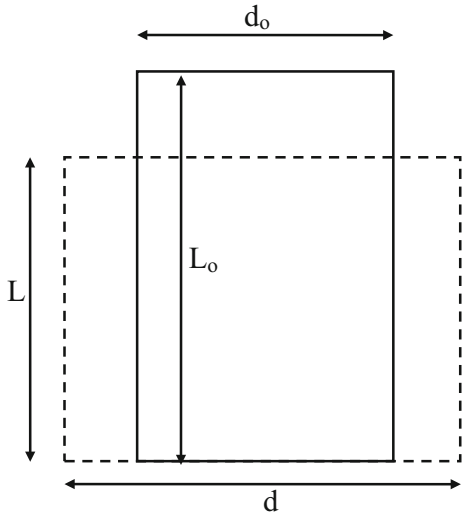

Fig. 12 Deformation of a triaxial soil sample without volume change

Strength of Geocell Reinforced Granular Soil

All the previous analyses are performed with planar reinforcement layers. The strength improvement is due to the surface friction developed along the interfaces. At low embedment depths, the reinforcement will undergo premature pullout type failure due to low confining pressures. In such cases, 3-dimensional form of the reinforcement is more appropriate. Geocells provide all round confinement to the soil irrespective of the surface pressures. Hence, the geocell reinforcement of soils is preferred in case of pavements or load bearing yards, etc.

The strength of the geocell reinforced granular soils was investigated by Bathurst and Rajagopal [9] and Rajagopal et al. [10] based on the analogy of rubber membrane theory developed by Henkel and Gilbert [25] for the analysis of strength of soft soils under triaxial compression.

For the purpose of simplified analysis, it was assumed that the cylindrical shape of the soil sample is preserved and it deforms without any volume changes as illustrated in Fig. 12.

If the volume of the soil sample remains constant during the test,

$$\frac{\pi}{4} d_o^2 L_o = \frac{\pi}{4} d^2 L$$
$$\therefore d = \frac{d_o}{\sqrt{L/L_o}} = \frac{d_o}{\sqrt{1-\varepsilon_a}} \tag{10}$$

Then the circumferential strain (ε_c) can be calculated as,

$$\varepsilon_c = \frac{\pi d - \pi d_o}{\pi d_o} = \frac{d - d_o}{d_o} = \frac{1 - \sqrt{1-\varepsilon_a}}{\sqrt{1-\varepsilon_a}} \tag{11}$$

Then the additional confining pressure due to the membrane stresses can be written as [25],

$$\Delta\sigma_3 = \frac{2M\varepsilon_c}{d}\frac{1}{(1-\varepsilon_a)} = \frac{2M}{d_o}\left[\frac{1-\sqrt{1-\varepsilon_a}}{1-\varepsilon_a}\right] \tag{12}$$

Table 1 Different series of triaxial compression tests performed

Type of reinforcement	Configurations of cells	Aspect ratio of cells (h/d_o)
Unreinforced	–	–
Woven geotextile (white)	Single	2
	Double	4
	Three	4.3
	Four	4.83
Woven geotextile (black)	Single	2
Nonwoven geotextile	Single	2
Soft mesh	Single	2

in which ε_a is the axial strain at failure, d_o is the initial diameter of individual cell pocket, and M is the secant modulus of the membrane of the cell at the axial strain of ε_a.

The shear strength of the sand encased with single and multiple geocells was investigated in [10]. The tests were performed with different types of geosynthetics and geometries as described in Tables 1 and 2. All the tests were performed on 100 mm diameter and 200 mm high soil samples encased in single and multiple geocells.

These geocells were hand made by stitching of woven geotextile. Schematic of the test configurations is shown in Fig. 13. A photograph of the soil sample with four geocell pockets is shown in Fig. 14. As the number of geocell pockets was increased, the strength of the soil sample was found to increase. However, beyond four pockets, the strength of the soil did not change appreciably as shown in Fig. 15. The data shown in this figure was obtained at 100 kPa confining pressure. Similar behaviour was observed at all the other confining pressures.

The failure in both the single and multiple geocell cases was observed to be by bursting of the seams at the mid-height of the samples. The seam strength was much lower than that of the parent geosynthetic material leading to the failure at the seams. In the case of samples with multiple geocells, the bursting has started from the seams of the outer cells and has slowly propagated towards the inner cells. Whereas the seams of the outer cells have showed clear rupture, the seams of the inner cells were damaged to a lesser extent.

The failure pattern of the samples encased in the geocells made of nonwoven geotextile and soft mesh was very much similar to that of unreinforced soil samples because of the excessive stretching of these geocells. Because of the low stiffness of these meshes, the geocells underwent such large lateral expansions that effectively the soil may not have been confined by these geocells at all.

The p–q diagrams constructed from test data on different samples are shown in Figs. 16 and 17 for different types of geosynthetics and different number of geocell pockets. The p is the mean normal stress defined as $(\sigma_1 + \sigma_3)/2$ and q is the shear stress defined as $(\sigma_1 - \sigma_3)/2$. The frictional strength of all samples was found to be nearly 40.5°. The data clearly shows that the slope of the lines (frictional strength) does not change appreciably with geocell confinement. Similar observation was also reported in [9].

Comparing the cohesive strengths of the samples encased in single geocell (Fig. 16), it is clear that samples with stiffer geocells developed higher cohesive strength. The two samples with nonwoven geotextile and mesh reinforcement did not develop appreciable apparent cohesive strength due to the low modulus of these geosynthetic materials.

There is a significant increase in the value of the apparent cohesion when the number of cells was increased beyond one. However, when the number of cells was increased from three to four, there was only a marginal improvement in the strength. The increase in cohesive strength is only marginal in this case. As the number of cells was increased, more area of the soil is confined by the cell pockets (Fig. 13) i.e. confinement offered by cells per unit volume of soil increases as the number of cells increases. However, this increase in unit confinement has not resulted in progressive increase in the apparent cohesion of soil as illustrated in Fig. 17. This result cannot be attributed to the changes in aspect ratio, as the change is only marginal, Table 1. This result can only be explained from the interaction that takes place between the different cells. The test results indicate that the improvement in the performance due to this interaction is not significant beyond three cells. Hence, we may conclude that the strength behaviour of three inter-connected cells may

Table 2 Types of geosynthetics used in the test series

Type of Geosynthetic material	Wide width tensile strength (kN/m)	Seam strength (kN/m)	Strain at peak strength (%)	Secant modulus of seam at 5% strain (kN/m)
Woven geotextile (white)	65	8	10	70
woven geotextile (black)	54.5	7.5	12.5	50
Nonwoven geotextile	9	9*	>30	5
Soft mesh	1	1*	>50	0.5

* seam intact - rupture in parent material

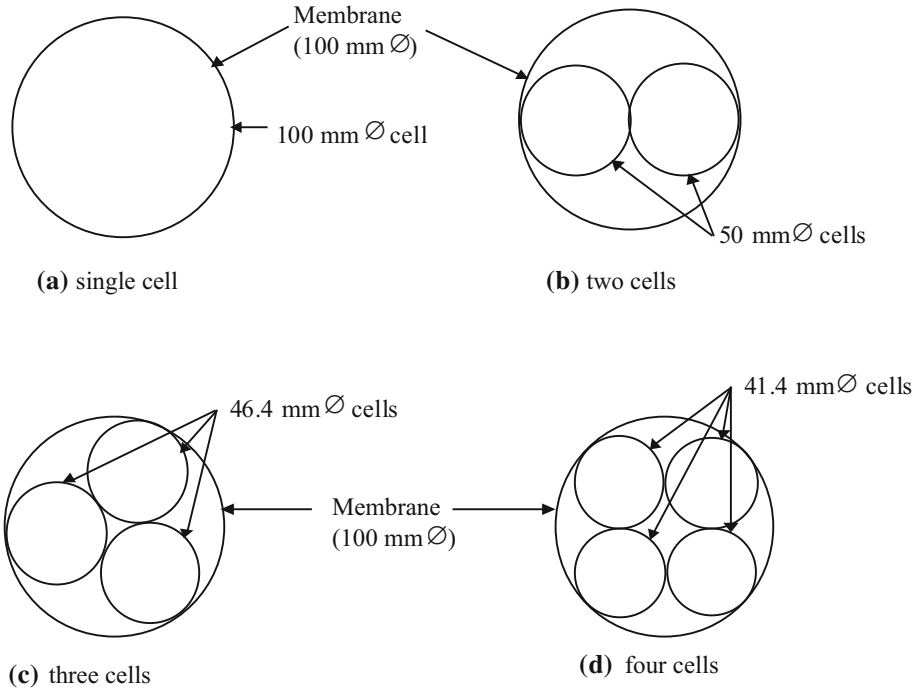

Fig. 13 Soil samples encased in *single* and *multiple* geocell pockets [26]

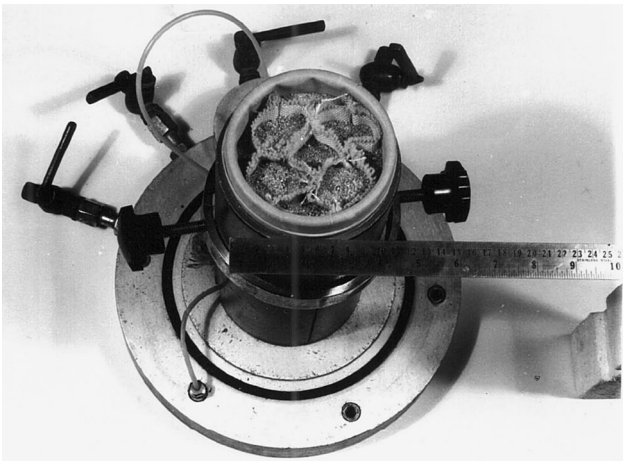

Fig. 14 Photographic view of the sand sample in *four* geocell pockets [26]

represent the mechanism of geocells having a large number of interconnected pockets.

The strength of the geocell reinforced granular soil can be understood to be due to development of apparent cohesion. The apparent cohesion for different configurations was estimated from the above equations using the relevant modulus of geosynthetic, geometric properties of geocell pockets and the axial strain levels developed during the laboratory tests. These estimated values (Eqs. 11, 12) are compared to those measured from the test data in Table 3. The axial strain corresponding to the peak deviator stress was used in these calculations. It is seen that the comparison is fairly accurate within the experimental variations. Hence, the theory described above may be assumed to be valid for geocell reinforced soil. The validity of the above equation for wide range of aspect ratios in the range of 1 to about 5 has been established in [9, 10].

In addition to the increase in the strength of the soil, there was a corresponding increase in the stiffness of the geocell reinforced soil, which is indicated by steeper stress–strain curves (Fig. 15). Because of the additional confining pressure on the soil due to the membrane stresses, the peak stresses occurred at larger strains. This is similar to the unreinforced soils developing peak stress at higher strains at higher confining pressures. As the number of cells was increased the stiffness of the soil sample has also increased. The stress–strain response of samples with three and four geocells was found to be almost identical (Fig. 15). Hence, we may once again conclude that the use of three interconnected cells in the model tests is adequate to represent the stiffness behaviour of geocells with many interconnected cells. More details of this research can be found in [26].

Latha [26] and Latha et al. [27], etc. have extended the above analyses to develop equations to obtain the modulus of the geocell reinforced soil layers. Successful back-predictions of the experimentally observed behaviour of strip footings and embankments resting on soft clay soils were obtained using these relations for modulus of geocell reinforced soils [26–31].

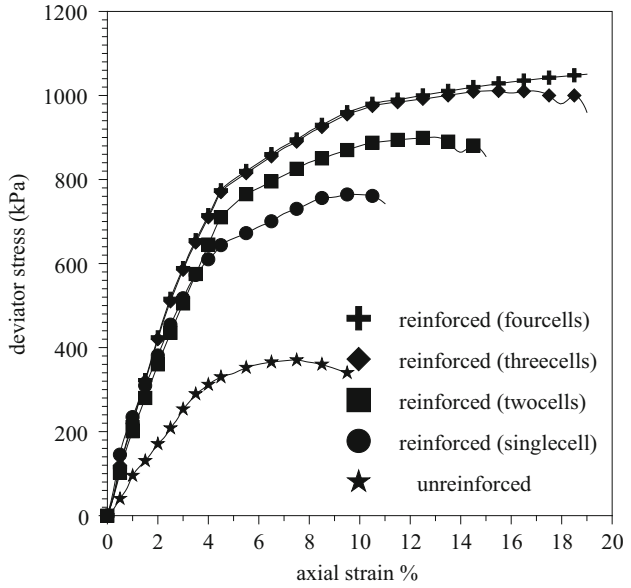

Fig. 15 Stress–strain response of soil sample with different *number* of geocell pockets [26]

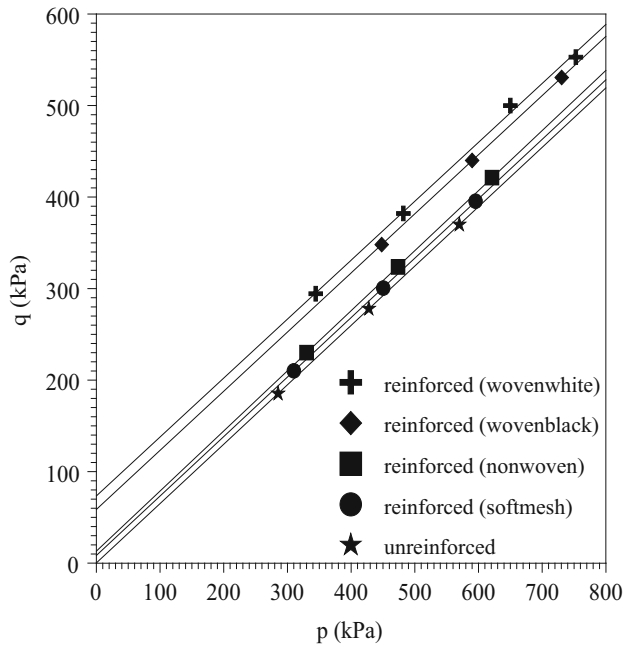

Fig. 16 p–q diagrams for tests with single geocell and different types of geosynthetics [26]

Construction of Reinforced Soil Retaining Walls and Slopes

Over the past three decades starting from the middle of 1980's, geosynthetics have been extensively used for construction of various types of structures like retaining walls, steep slopes, landfills, coastal erosion protection structures, etc. A few of these projects are described in this section to give an overview of geosynthetic applications in India.

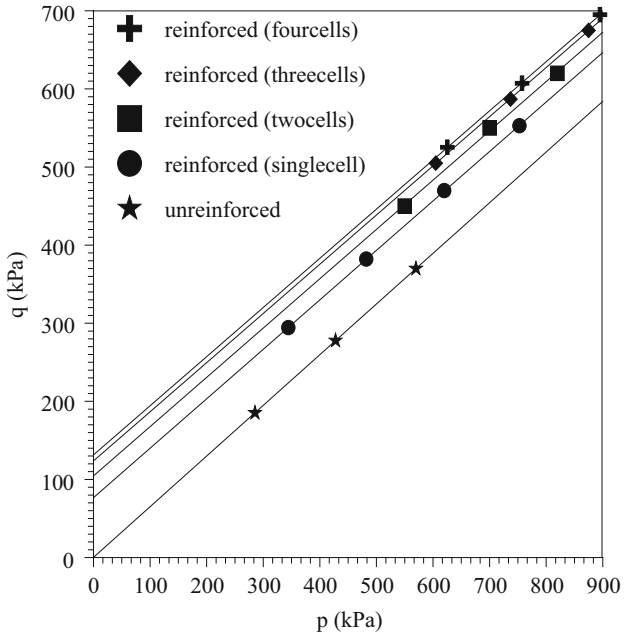

Fig. 17 p–q diagrams with different *number* of geocell pockets and woven geotextile [26]

Table 3 Comparison of measured and predicted cohesion values

No. of cells within the test	Theoretically Estimated cohesion (kPa)	Experimentally determined cohesion (kPa)
Single		
Woven-white	92.0	98.9
Woven-black	80.0	77.0
Nonwoven	14.6	17.4
Woven-white		
Two	128.8	134.8
Three	182.2	159.2
Four	189.8	169.1

Construction of Tiered Reinforced Soil Retaining Walls

Recently, two steep vertical walls of 22.5 and 41 m high were built at Vijayawada, AP which are among the highest such walls in India and the world [32, 33]. These walls were constructed to widen narrow sections of a ghat road leading to a hill-top temple and also to create large parking area for vehicles at the top of the hill. The original ghat road was quite narrow as illustrated in Fig. 18.

The specific conditions at the site are: the hill slopes are quite steep and fragile, access to the construction site is

Fig. 18 Typical *narrow* section of ghat road at Vijayawada

limited and the level difference between the ground level and the ghat road level is quite high. The difficult access of the site and the tight working space eliminates many of the conventional construction methods such as construction of reinforced concrete walls or column supported platforms, etc.

As an alternative, reinforced soil technology was explored for the construction at the site. The reinforced soil retaining walls consist of thin facing elements which are provided to prevent soil erosion and for aesthetic purposes, some length of flexible polymeric reinforcement to take care of lateral stresses in the soil. These reinforcement layers are similar to the steel reinforcement provided in the reinforced concrete. Among the different reinforced soil wall technologies, the one that employs pre-cast modular block system was adopted for ease in handling. The facing elements used at the site were modular blocks similar to rockwood blocks having mass of approximately 35 kg, shown in Fig. 19. These blocks are of length 450 mm on the front side and 350 mm on the backside. The height of each block is 200 mm. These blocks are manufactured by cold pressing process with cement concrete having minimum compressive strength of 35 MPa after 28 days curing.

The configuration adopted was tiered configuration for ease of construction, aesthetic appearance and ease in maintenance operations. The wall sections were designed as per the relevant design codes [17, 34]. The design guidelines for tiered walls are rather limited. The FHWA [18] suggests that the tiered soil retaining walls could be designed using slip circle analysis to achieve the minimum required overall stability against failure. The schematic sections of the 22.5 and 41 m high walls are shown in Figs. 20 and 21. The bottom tier was 12 m high and the upper tier was 10.5 m high in the 22.5 m high wall.

Fig. 19 Modular facing block used for construction of retaining walls

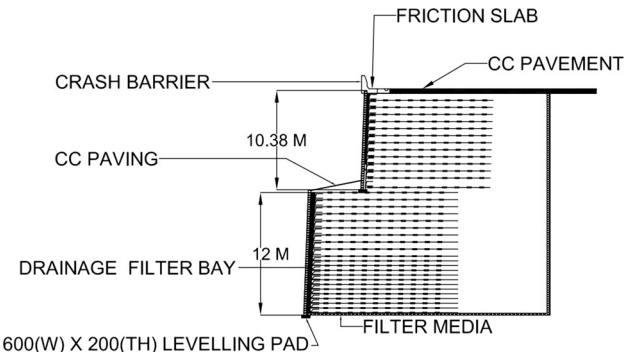

Fig. 20 Cross-section of the 22.5 m high wall

As these walls were constructed abutting steep hill slopes, large runoff water may enter into the backfill soil in these walls. In order to prevent the water from entering the backfill soil, good drainage was provided over the full-height in the form of chimney drains. The chimney drain consisted of uniformly graded coarse aggregate of 300–500 mm thickness below and immediately behind the infill soil as illustrated in Figs. 20 and 21 and the photograph in Fig. 22. The reinforcement layers provided were of geocomposite type that can act as both reinforcement layer and also as drainage and filtration layer.

The reinforcement layers of different strengths ranging from an index tensile strength of 50–200 kN/m were used in the construction and the corresponding long term allowable design strengths ranged from 29 to 115 kN/m. The wall has been checked for both external and internal stability. The lengths of the reinforcement layers for both upper and lower tiers were determined through external stability calculations, viz. sliding, over-turning and bearing failures. The vertical spacings of the reinforcement layers were determined through internal stability calculations, viz. pullout and rupture considerations. Further, the force in each reinforcement layer was also verified against the connection strength at that depth. The connection strength between the facing blocks and the geosynthetic was purely mobilized by friction. The connection strength was

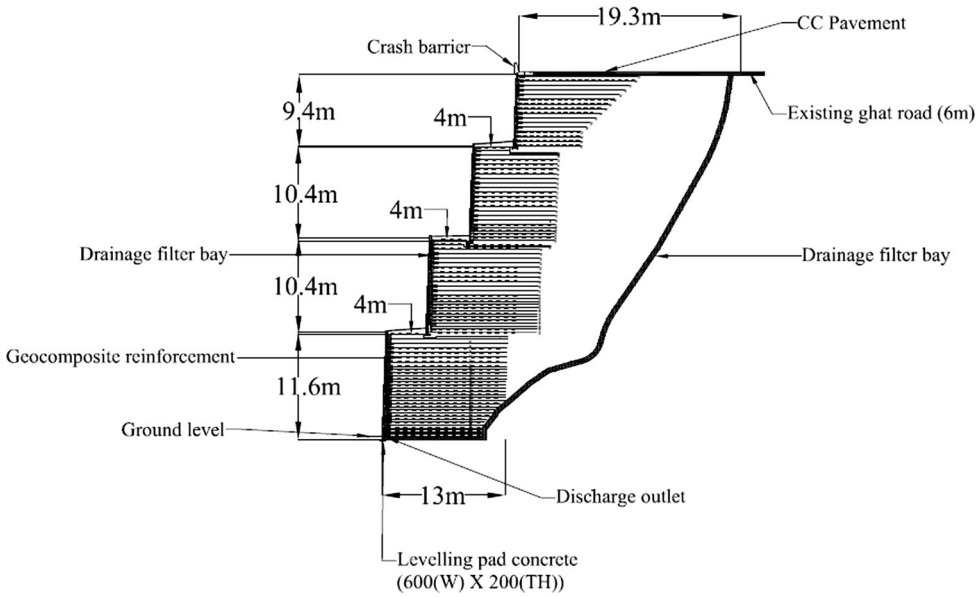

Fig. 21 Cross-section of 41 m high retaining wall

Fig. 22 Close up view of chimney drain and the geotextile filter

determined by performing large-scale laboratory tests at IIT Madras as per the ASTM code procedures [35]. Typical data obtained from such connection strength tests for a geocomposite having index tensile strength of 75 kN/m is given in Table 4.

Apart from all the static loads, the design has also considered the seismic loads as per the site specific conditions (Zone-III). The final designs were verified by stability analysis performed using two different softwares RESSA and TALREN. Both are industry standard programs for design and analysis of reinforced soil slopes. The results from the slope stability analysis of 2-tier wall and 4-tier walls are shown in Figs. 23 and 24. The minimum factors of safety for both cases exceeded 1.30 even after including the seismic forces. Hence, the designs are satisfactory.

Table 4 Typical data from connection tests

Normal load (kN/m)	Approx. wall height (m)	Load at 20 mm displacement (kN/m)	Peak load (kN/m)
10	1.90	12.6	15.5
15	2.80	14	17.2
20	3.75	15.5	19.4
25	4.70	17.1	22.3
30	5.60	18.5	23.8
35	6.6	19.4	25.3
40	7.5	20.7	26.9
50	9.35	23.4	28.8

Pictures of the construction site during the construction progress are shown in Figs. 25 and 26. Notice that there is no access from external side once the walls reach a certain height. All the compaction equipments moved up along with the backfill soil and finally came out from the construction site after reaching the level of ghat road. All the soils required for the construction were dumped from the ghat road. The backfill soil used is a mix of imported murum soil and river sand. The compaction quality was monitored carefully at each level. The entire construction site was covered with polythene sheets during even light rains to prevent mixing of water with the soil.

A view of the ghat road with widened road and a picture of the 2-tier wall taken from the Krishna river are shown in Figs. 27 and 28. An overall picture of the 41 m high 4-tier wall and the additional parking space gained are shown in Figs. 29 and 30.

The construction of 22.5 m high wall was completed in October 2008 and the 41 m high wall was completed by the

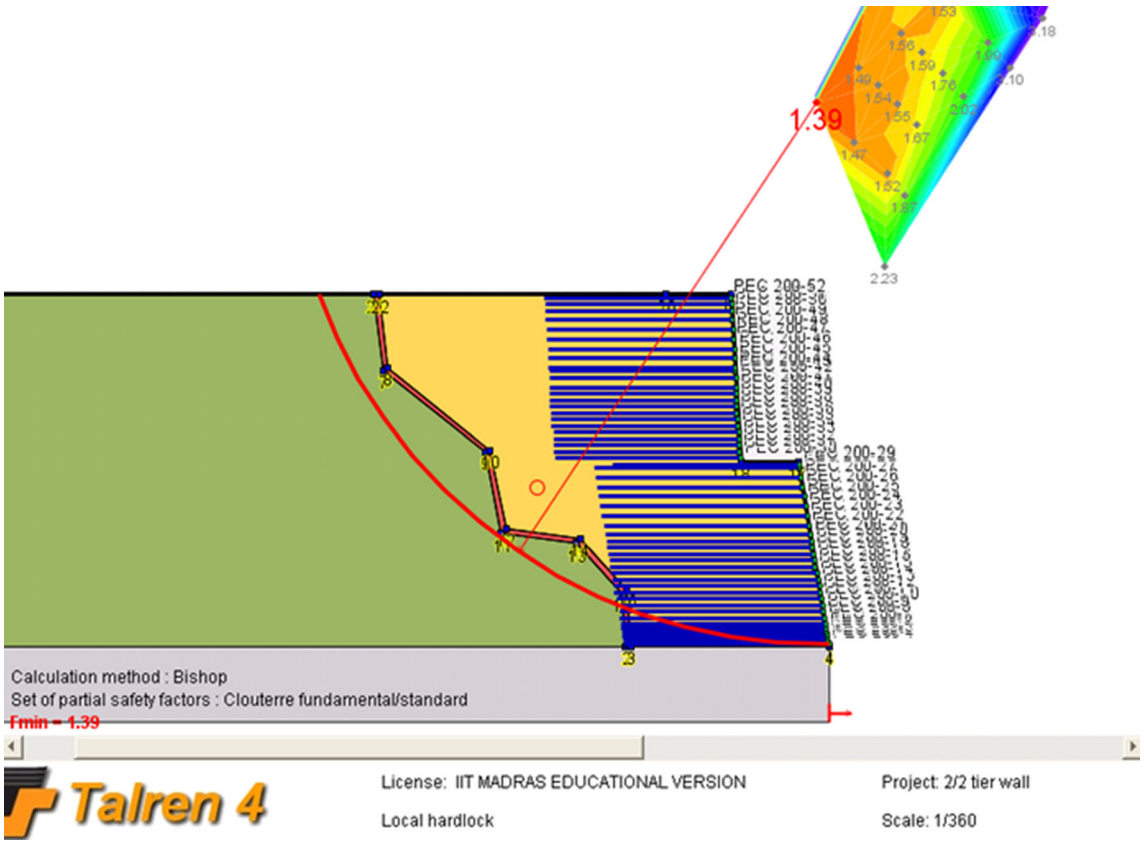

Fig. 23 Results from slope stability analysis of 2-tier slope by TALREN program

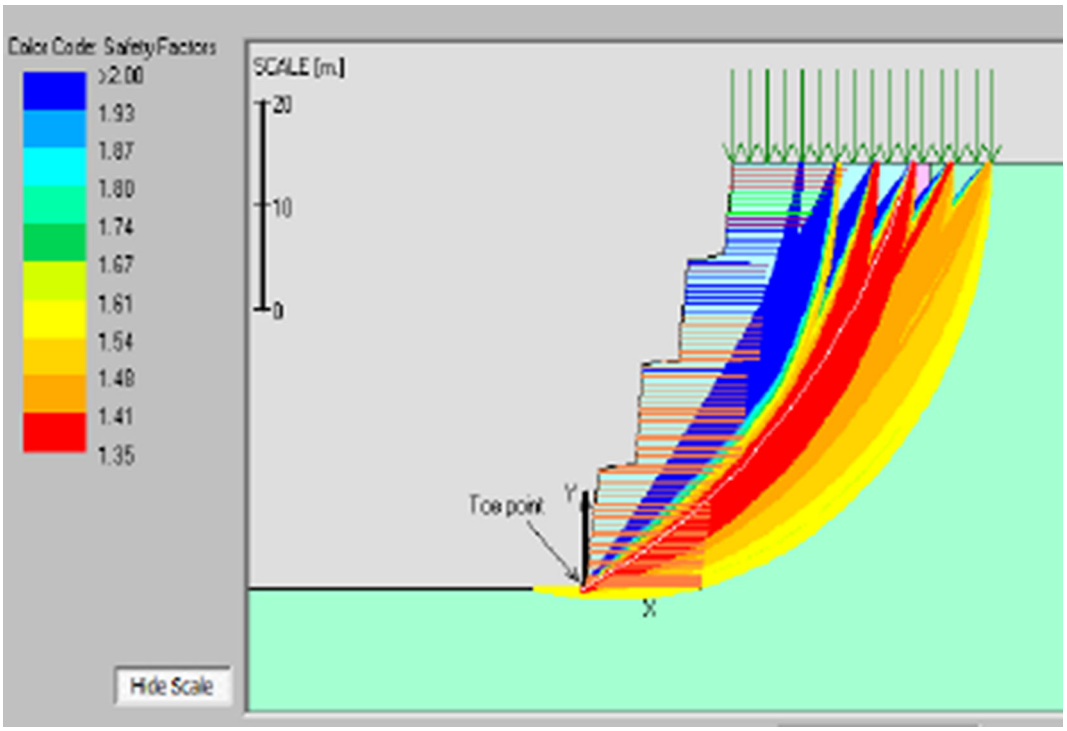

Fig. 24 Results from stability analysis of 4-tier slope by RESSA program

Fig. 25 Laying of the blocks

Fig. 26 View during mid-way height

Fig. 27 Widened ghat road

Fig. 28 22.5 m high wall

Fig. 29 Overall view of 41 m high wall

Fig. 30 Extra space created for parking

Fig. 31 Relative settlement at interface at hill soil

end of the year 2009. Both walls were continuously monitored for their performance. The 2-tier wall did not undergo any significant lateral or vertical deformations. The backfill soil behind the 4-tier wall had undergone a settlement of the order of 500 mm. Some bulging at the 2nd and 3rd tier levels was noticed. Some part of the upper tiers of the wall was built on the soil in lower tiers while the remaining part was built directly on the hill slopes. Hence, there were relative settlements along this interface which lead to some cracking of facing blocks as illustrated in Fig. 31. In hindsight, it appears that a vertical construction joint should have been provided at this location to prevent such response. In any case, all the deformations have stabilized within the first 2–3 years of service. There are no further deformations either horizontal or vertical. The parking lot at the top of the hill is thrown open for regular operations.

These two walls were built within the budget and time limits. In fact, the 2-tier wall was completed at least 6 months before the scheduled completion time. The settlements in the 4-tier backfill soil could be due to quick constructions without allowing for settlements under its own weight of 41 m of soil.

Construction of Pakyong Airport Embankment at Gangtok, Sikkim

One of the most challenging geosynthetic projects is the construction of airport runway at Pakyong, Sikkim. In order to create a long level ground in extremely hilly terrain, some parts of the hill slopes on one side of the runway had to be cut and the same soil used for filling of deep valleys on the other side of the runway at the airport site [36–38], Fig. 32. The total earthwork volume handled at the site is nearly 6.5 million cubic meters to cut the hills and fill the valley portions (Fig. 33).

The total length of the developed level ground was approximately 1800 m in length and 150 m wide to accommodate the runway and other airport related structures. The cut slopes on the hill side had a height of around 100 m while the height of soil to be retained on the valley side ranged from about 30 m to 74 m to a total length of nearly 1500 m. The major problems to be overcome at the site include the extremely hilly terrain where heavy equipments cannot be moved easily, heavy rainfall intensities, seismic activity, fragile ecological system, etc. The average annual rainfall at the airport site is very high at about 4000 mm and hence the retaining structures should be highly permeable and sufficient surface and sub-surface drainage has to be provided to deal with the huge quantities of flow. Coupled to these, another major hurdle is that 9 streams (Jhoras) flow across the proposed runway length on which the local people on the downstream side depend for their water supply needs. Hence, the runway structures

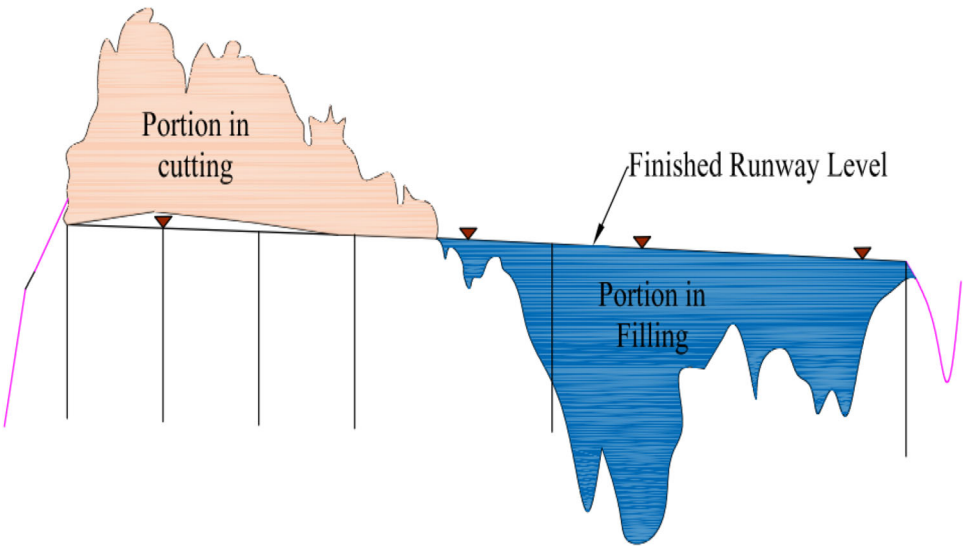

Fig. 32 Schematic of cutting in hill portion and filling of valley portions [37]

Fig. 33 Stone filled gabions as facing elements [36]

should not hinder the flow of water into or through these streams under any circumstance.

The only possible solution to tackle heavy rainfall and high seismic activity is to use flexible and permeable retaining structure to address both the issues. The reinforced soil structures are highly flexible which can withstand the seismic inertial forces effectively. The solution adopted at the site is to use stone filled gabions as facing elements and very high strength geogrids made of polymeric strips as reinforcement elements. The cut hill slope surfaces were covered with coir mats to promote quick growth of vegetation and prevent erosion during rainfall. Very high strength geogrids having tensile strengths in the range of 200–800 kN/m were used as primary reinforcement layers. The gabions boxes were metallic double twisted wire net gabions with short length of wire net that acts as secondary reinforcement. The gabion boxes were filled with stones and soil to promote the growth of vegetation on the wall surface that adds to the stability, reduces erosion potential and also blends the structure with the green surroundings. The vertical spacing of the reinforcement layers was nearly 2 m which is more than the code provisions of 800 mm. This is to allow for speedier constructions in view of short construction windows.

The flow through the streams was channelized into lined canals and allowed to pass under the runway structure through RCC box culverts designed to carry the estimated flow quantities. The outlet of these culverts at the other side of the runway was stepped made out of stone filled gabions to reduce the energy of the flowing water. The three most critical elements of the design are "drainage, drainage and drainage". Hence, utmost care was taken by providing geosynthetic drainage blankets and filters at all the critical locations of the project. Full video presentation on the construction details could be found at http://www.nptel.iitm.ac.in/courses/105106052.

The retaining structure at the site had successfully withstood the 6.8 magnitude earthquake in September 2011. While the structures in other areas had suffered damage and the earthquake had induced severe landslides at other locations, the airport structure could stand without any damage. The drainage arrangements in the structure were also found to function smoothly. The Pakyong airport is scheduled to open for commercial operations in the year 2017. The airport embankments at this airport was designed and constructed by M/s Maccaferri Environmental Solutions Pvt. Ltd (India).

Very High Reinforced Soil Embankment for Bypass Road at Shillong

The construction of a bypass road at Shillong required the construction of an embankment of height up to 38 m. This bypass road connects two national highways NH-40 and

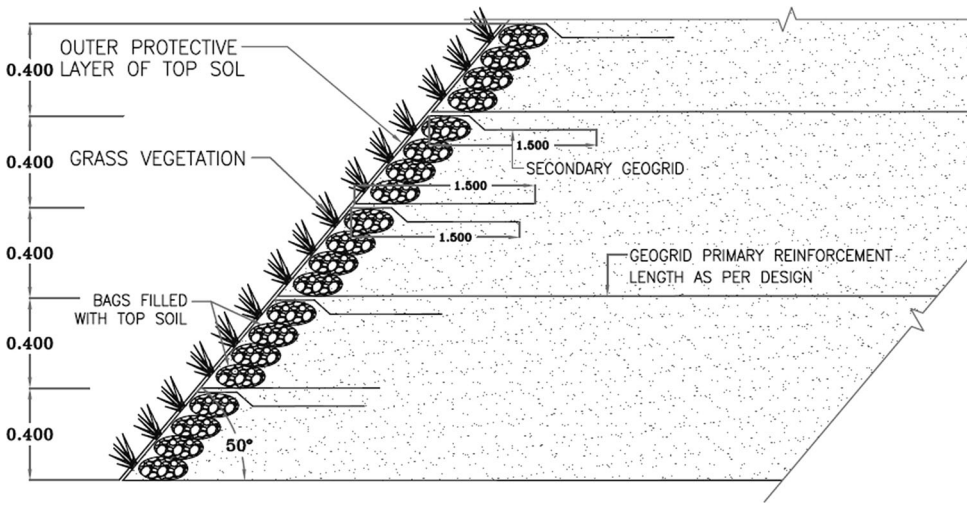

Fig. 34 Schematic of the reinforced soil embankment at Shillong

Fig. 35 Tiered embankment during construction

Fig. 36 Close-up view during construction

NH-44 in Shillong city in the state of Meghalaya. The site conditions are characterized by heavy rainfall, high seismicity (Zone-V), hilly terrain, etc. The drainage and soil erosion are major issues to be considered while planning the construction for this structure also. Based on the space availability and economy of project, it was decided to construct a soil embankment at 50° slope angle with reinforcement layers. The front face of the embankment was protected by sand bags and the reinforcement layers were wrapped around these bags. The bags are filled with vegetated soil to promote the growth of vegetation. The primary reinforcement layers were provided at 800 mm vertical spacing while secondary reinforcement layers were placed at every 400 mm. The schematic of erosion protection and the reinforcement details are shown in Fig. 34.

The reinforcement layers consisted of polyester geogrids having ultimate tensile strengths in the range of 60–120 kN/m. Typical length of reinforcement layers varied from 10 to 20 m depending on the height of the

Fig. 37 Completed slope with road traffic and surface vegetation

slope. The vertical spacing and lengths of reinforcement layers were designed to achieve a minimum factor of safety of 1.3 under static loading and 1.1 under seismic loading. The entire height of embankment was constructed in tiers to reduce the erosion potential of surface runoff. The drainage issues were addressed by placing stone aggregate as chimney drains behind the backfill soil and also below the soil at the base. At periodic vertical and horizontal intervals, perforated PVC tubes were provided to drain the backfill soil. Some pictures of the soil embankment during the construction and service are shown in Figs. 35, 36 and 37. The bypass road was opened for traffic about 2 years back and is in service now.

Construction of Runway at Kannur International Airport

Very similar structure to the above constructions is being constructed at Kannur, Kerala with slightly less severe challenges. This embankment is to support part of the airport runway at Kannur international airport, Kerala. This is the first such project where the designs were vetted by finite element analysis upon the insistence of proof consultant. The total height of the slope ranged from approximately 66–87 m. The entire height was split into a bottom relatively shallow slope and steep top slope portion Fig. 38.

Both the bottom and top parts of the slope are provided with reinforcement layers. The angle of the bottom slope ranged from 26° to 41° while that of the top slope ranged from 43° to 65° at different chainages. The soil used at the site is relatively marginal lateritic soil that has excellent properties when dry and hs tooth paste consistency when wet. The slopes were designed with a small cohesion of 10 kPa and friction angle for the soil as 30°. The slope was designed as a reinforced soil slope to achieve a factor of

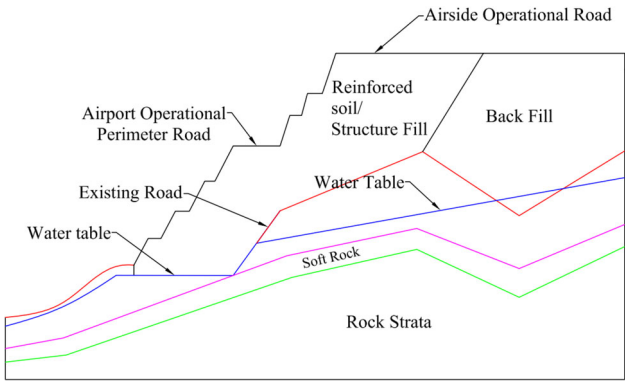

Fig. 38 Schematic of the slope proposed at Kannur international airport

safety of 1.3 under static loading and a factor of safety of 1.0 under seismic conditions with a horizontal seismicity factor of 0.096. Typical critical slip surfaces are shown in Fig. 39. The geosynthetic reinforcement layers had short term tensile strengths ranging from 50 to 1350 kN/m. The primary reinforcement layers were provided at 800 mm vertical spacing. Secondary reinforcement layers of short length were provided at every 400 mm vertical intervals. The length of the primary reinforcement layers had exceeded 40–45 m at some elevations due to the complex geometry of the construction, Fig. 40. The surface of the soil in slope is protected from erosion by coir mat and growth of vegetation (Figs. 41, 42). The subsurface water was prevented from entering the reinforced fill soil by providing a chimney drain of 600–900 mm thickness behind the reinforced soil fill. The water is lead out of the embankment by providing a thick drainage blanket at the bottom of the fill soil. The surface of the soil at the top of the embankment was also provided with erosion control mat and a highly permeable surface drain to prevent the surface water from percolating into the reinforced soil fill.

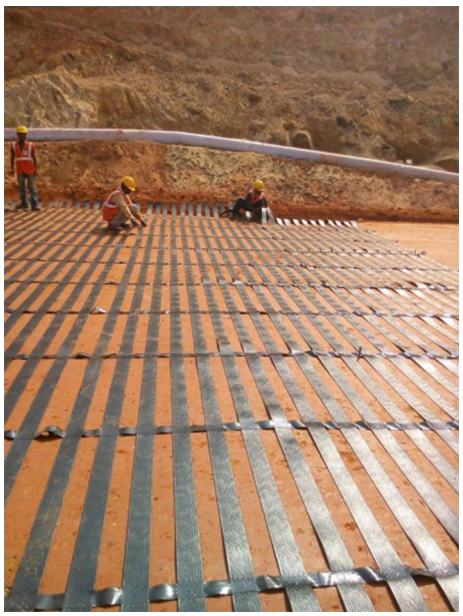

Fig. 40 View of polymetric strip reinforcement and chimney drain at back end

Construction of Hazardous Waste Landfills Using Geosynthetics

The introduction of geosynthetics has facilitated the construction of safe disposal grounds for storing hazardous wastes. The leachates produced by the reaction of the wastes with water should not migrate from the landfill and contaminate the ground water. Hence these landfills are scientifically designed and carefully constructed to minimize the leakage. Traditionally thick layers of compacted clay layers are used as effective barriers against fluid transmission. However, the clay soil may undergo cracks due to both swelling and shrinkage leading to possible leaks. To prevent the continuity of cracks through the

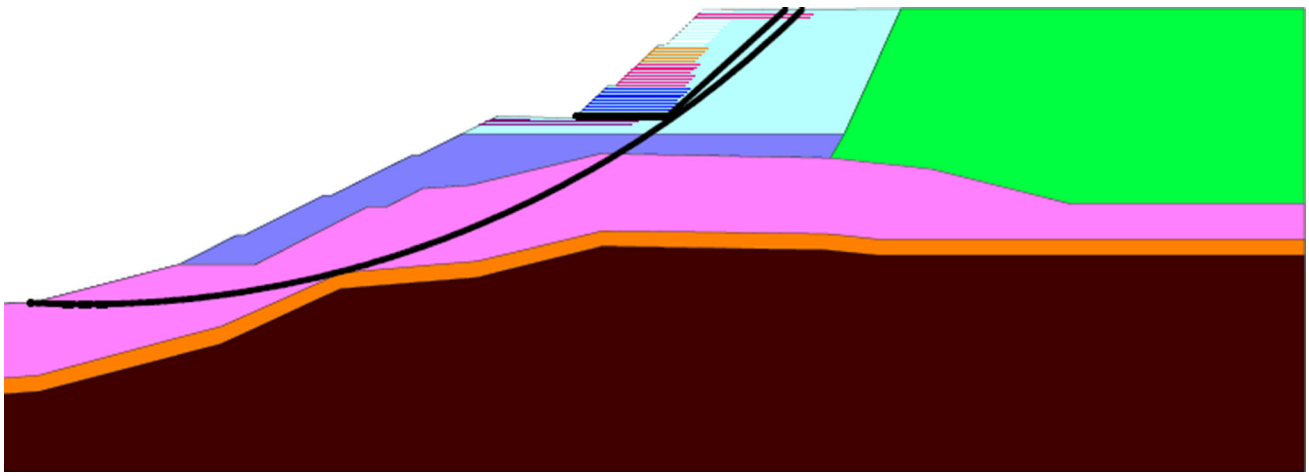

Fig. 39 Critical slip *circle* and sliding surface from the slope stability analyses

Fig. 41 Toe protection using gabions and surface erosion control measures

Fig. 42 Close-up view of biomat for growth of vegetation on slopes

thickness (and prevent leakage), large thicknesses of clay layer are usually provided. However, if the thickness of the clay layer is large, effective storage capacity of the landfill decreases.

With the introduction of geosynthetics, the safe construction of the landfills has increased manifold. The geomembranes are used as tight barriers, geosynthetic clay liners (GCLs) are used to repair any cracks that may happen in geomembrane or clay layer, thin geonets are used as drainage layers in place of thick sand layers to collect the leachate, geotextiles as drainage or protection layers, geogrids to increase the slope angles of the landfills. The landfills provide the largest number of applications for the use of geosynthetics. The self-healing properties of the GCLs were investigated by Sivakumar Babu et al. [39].

The first major landfill that was built in India (in the year 2002) was at Hindustan Zinc Factory, Visakhapatnam [40]. This was built to store the hazardous waste of Jarosite

Fig. 43 Overall view of the landfill at HZL, Visakhapatnam

Fig. 44 Geogrid reinforcement in landfill embankment

which is a by product of the zinc smelting process. This is an above ground landfill due to the presence of hard rock at shallow depths. The landfill was created by constructing 10 m high bunds all around and lining the inner surface with 2 mm thick geomembranes. The length of the landfill is approximately 280 m and width of 210 m on one side and 110 m on the other side, Fig. 43.

The landfill is constructed using granules of the Jarosite waste to save the storage space in the landfill. As the Jarosite granules had very low frictional strength (<30°), the slopes had to reinforced with geosynthetic layers. The slopes were reinforced with welded geogrids having tensile strengths in the range of 50–150 kN/m at vertical intervals of 600 mm, Fig. 44. Nonwoven geotextiles were used as wrap around facia (Fig. 45) for the slope surfaces. A 8 mm thick nonwoven geotextile was used as cushion below the geomembrane layer to prevent punching failure. The geomembrane was overlain by a 10 mm thick geotextile and a geonet as drainage layer. This was covered with the second 2 mm thick geomembrane layer and a 10 mm thick geotextile. Finally, the slopes were covered by interlocking cement blocks. The geomembranes were joined along the slope by hot wedge

Fig. 45 Wrap around facing of slope surface covered with coir mat

welding and the weld quality was vacuum tested during the construction as illustrated in Fig. 46.

The bottom of the landfill consisted of 600 mm thick compacted clay liner above prepared subgrade. Above this clay layer 300 mm thick sand layer and 2 mm thick geomembrane followed by another layer of sand and geotextile were provided. Leachate collection system consisting of highly permeable sand layers, geonet and perforated pipe lines was provided at the base and on all four sides of the embankment bunds. The collected leachate was diverted to a treatment plant. The Jarosite sludge was pumped back to the landfill while the treated water was let off. The ground water around the periphery was continuously monitored for any leakage of contaminants. The landfill was filled to capacity and was finally capped (in the year 2010) to close the landfill, Fig. 47.

The landfill at HZL, Udaipur is also an above ground facility to store the Jarosite waste. The landfill was constructed initially in around 2006 with an initial height of slope of 11 m. This was later increased to 14 m during the period 2010–2011. As there was adequate space outside of the fill, the increase in height of embankment was achieved by using the down-stream method of construction. The outer slope was made steep at some locations by using reinforcement layers. As the full capacity was achieved, it was proposed to raise the height of the pond by another 2 m. In some stretches, the downstream method could be followed while in some sections, the height increase was achieved by using the upstream method. Both these techniques are illustrated in Fig. 48.

The upstream method of construction was found to be very difficult because of the soft nature of the sediments in the pond. Initially, the construction vehicles could not move due to the soft top surface. Geocells filled with stone aggregate and geogrid layers were used to improve the surface stiffness to be able to move the vehicles and

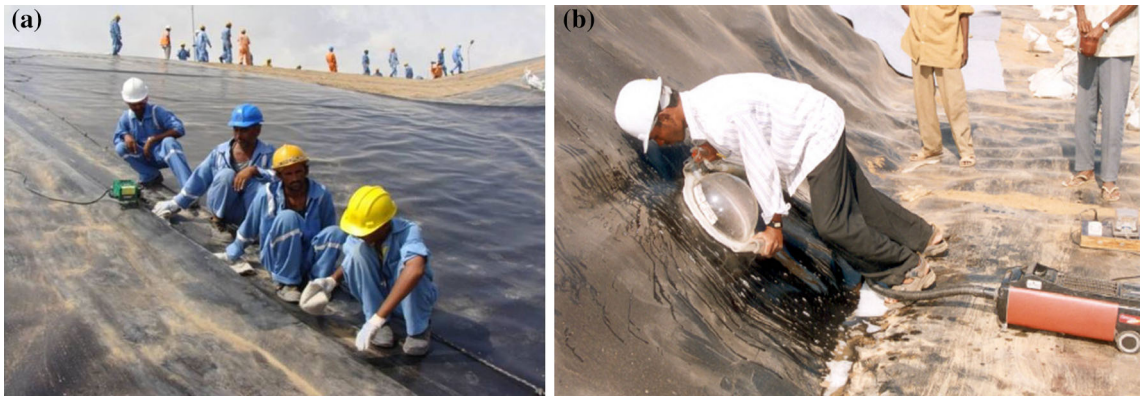

Fig. 46 Installation of geomembrane on the landfill at HZL plant. **a** Hot wedge welding, **b** vacuum testing of the weld quality

Fig. 47 Photographs of the HZL, Visakhapatnam landfill after capping. **a** Landfill full of Jarosite waste, **b** view of the capped landfill at HZL

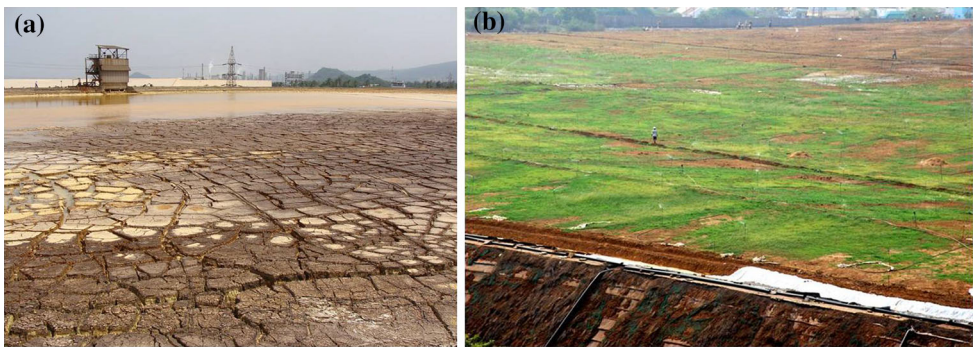

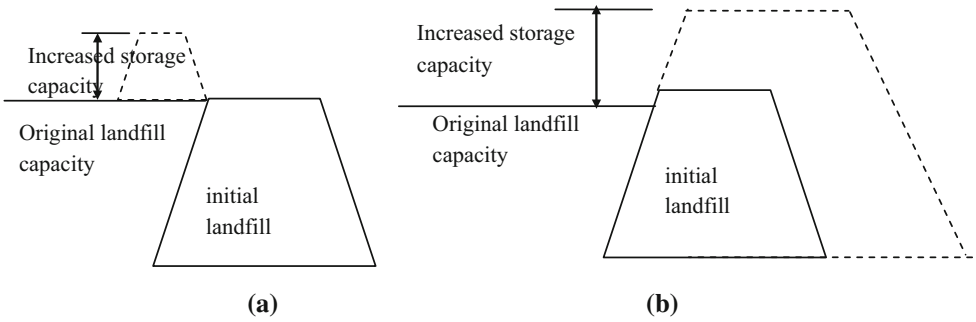

Fig. 48 Two methods for expanding the capacity of landfills. **a** Upstream method, **b** downstream method

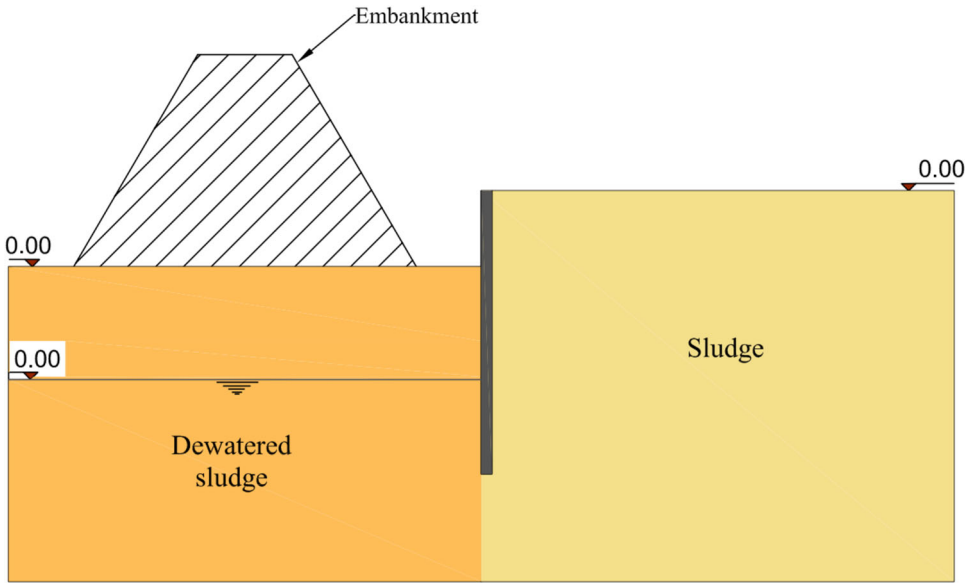

Fig. 49 Schematic of plastic sheet piling to reduce seepage

perform the construction operations. Plastic sheet piles were driven just ahead of the upstream slope to a depth of about 4.5 m below the surface to reduce the seepage into the slope as illustrated in Fig. 49. Photographs of the sheet piles and the geocell surface are shown in Fig. 50.

Another major challenge is to extend the geomembrane lining by welding to the pre-existing geomembrane layer. This was accomplished by carefully exposing the previously laid geomembrane, cleaning it and then laying fresh layer of geomembrane and welding it using hot wedge method. More details of this project can be found in [41].

Geosynthetic Solutions for Construction in Soft Clay Soils

The soft clay soils pose the most challenges to foundation engineers. Traditional geotechnical solutions for construction in these soils consist of granular columns or accelerated pre-consolidation using sand drains. With the advent of geosynthetics, there are wider solution options which could be more economical cost and time wise. Some typical conventional solutions and their geosynthetic equivalents are listed in Table 5.

The geosynthetics have been applied extensively in the Navi Mumbai area for development of road and rail net work and for erosion control. Detailed description of these can be found in [5, 6]. The following three popular geosynthetic based construction procedures are briefly discussed in the following sections.

Geosynthetic Encased Granular Columns

The granular columns (made of coarse sand or aggregate) are commonly used to support flexible structures like embankments, oil storage tanks, etc. These columns are known to improve the load bearing capacity and also reduce the settlements. The granular piles were first used in France around 1830's [42]. When the load is applied, the granular column bulges and gets lateral confinement from the surrounding soil in the form of passive pressure, thus forming a composite soil/granular column system [43, 44]. The load capacity of these columns and the reduction in settlements due to these columns can be estimated using standard procedures as given in IS code IS15284 [45].

Fig. 50 Photographs showing the plastic sheet piles and geosynthetic layers. **a** Plastic sheet piles, **b** geogrid and geocell layers

Table 5 Some typical approaches for construction in soft foundation soils

Sl. No.	Traditional solution	Geosynthetic solutions
1	Wide footings to reduce foundation pressure	Reinforced soil beds with multiple layers of reinforcement or use of geocell layers
2	Accelerated pre-consolidation using sand drains	Use of PVDs or vacuum induced consolidation
3	Granular columns	Encased granular columns
4	Pile raft foundations using reinforced concrete piles and raft	Geosynthetic reinforced load transform platform using cement concrete elements
5	Batter piles to support significant lateral loads	Vertical piles with horizontal geosynthetic reinforcement layers to support the lateral loads
6	Use of shallow slopes with berms	Steep reinforced soil slopes
7	Gravity retaining walls with strong foundation	Reinforced soil flexible retaining walls with wider reinforcement at base layers

The load bearing capacity of these columns is very much a function of the shear strength of the surrounding soil. The ultimate load carrying capacity of these columns is only 25 times the shear strength of soft clay [46, 47]. In the case of extremely soft clay soils with cohesive strengths less than 25 kPa, the formation of the column itself is doubtful and the load capacity may not develop fully due to the contamination of the aggregates with fine clay soil particles. Once the aggregate in the columns is contaminated, the load bearing capacity and the drainage capacity will reduce significantly leading to the ineffective columns. McKenna et al. [48] have reported the failure of a stone column treatment in soft clay soils due to the above reasons.

The geosynthetic encasement of the granular columns helps in the performance improvement in several ways. First, as the geosynthetic layer acts as a good separator and drainage layer, it will prevent the contamination of the aggregate with soft clay soil particles and helps in quicker dissipation of the pore pressures leading to better consolidation and strength [49–52]. The load capacity of the geosynthetic encased columns has been extensively reported in publications [53–60]. The geosynthetic encased granular columns have been applied for construction in soft clay soils in several projects [61–63].

The increased stiffness of the encased stone columns is known to promote higher load transfer into the granular columns and lesser load on the soft clay soil. This aspect was investigated by Murugesan [64] and Murugesan and Rajagopal [52] by performing load tests on group of encased stone columns as shown in Fig. 51. These tests were performed on soft clay soil having undrained cohesive strength of the order of 3–5 kPa. Large diameter steel plate that rests partly on three aggregate columns and partly on the clay soil was load tested. The pressure developed on the columns and the clay soil was measured using earth pressure cells having least count of 0.1 kPa.

The stress intensity factors for the ordinary stone columns and two types of geosynthetic stone columns and the clay soil is shown in Fig. 52. The woven geotextile is stronger and stiffer than the nonwoven geotextile encasement. The stress concentration factor is higher in the encased stone columns as compared to that of ordinary columns. Similarly, the pressure transferred into the clay

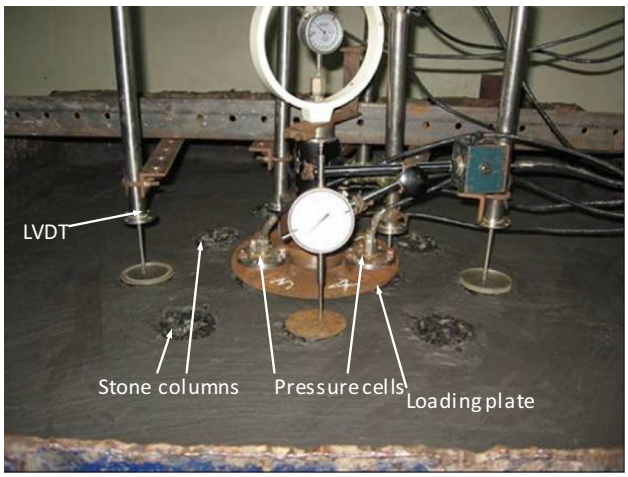

Fig. 51 Load tests on geosynthetic encased stone column–soil system [64]

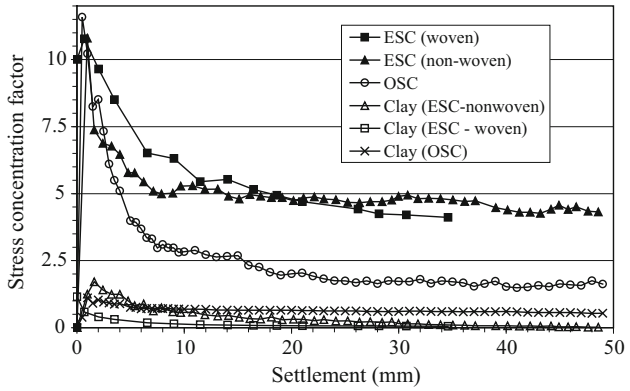

Fig. 52 Stress concentration on the stone column with settlement [64]

soil is lower with stiffer geosynthetic encased columns as shown in the figure.

The influence of the modulus of the geosynthetic encasement and the shear strength of the clay soil on the pressure–settlement behaviour was investigated by Murugesan and Rajagopal [49] through finite element analyses. The performances of the ordinary (OSC) and encased (ESC) stone columns were studied through axi-symmetric models and the results are shown in Fig. 53. The influence of the shear strength of the soil is significant on the pressure–settlement response of OSC and ESC with low encasement modulus. It could be observed that as the modulus of encasement is increased, the pressure–settlement response of ESC is not very much dependent on the shear strength of the clay soil.

They have attributed the influence of encasement to the increase in the confining pressure within the granular column due to the mobilization of hoop tension within the encasement. The influence of the encasement modulus on the confining pressures generated within the granular

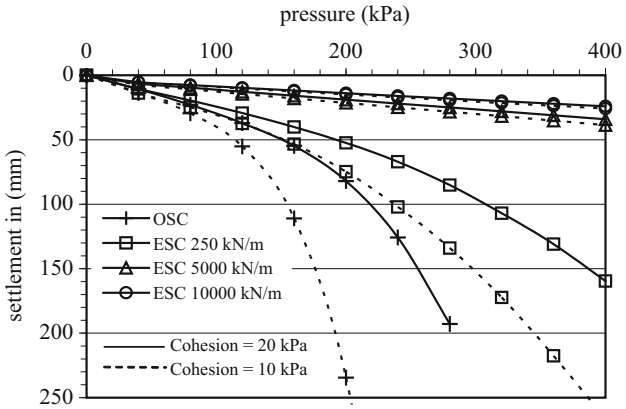

Fig. 53 Influence of shear strength of soil on the ESC and OSC [64]

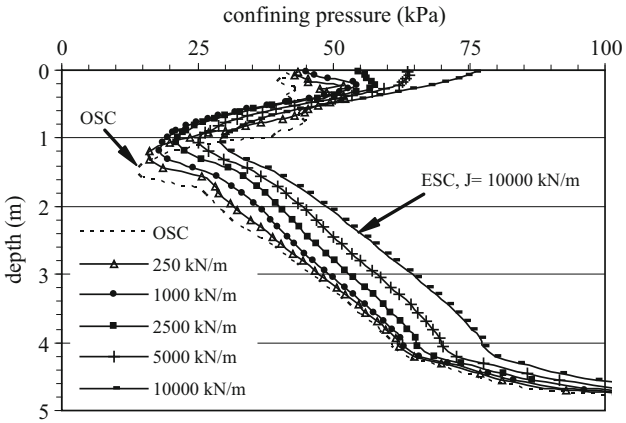

Fig. 54 Influence of encasement modulus on the confining pressures [64]

column is shown Fig. 54. It can be observed that the confining pressures within the OSC are close to those due to the at rest condition in the soil while the same in ESC increase with the increased modulus of the encasement material. The increase in confining pressure in the granular column leads to stronger and stiffer response of these columns as could be expected.

The influence of the geosynthetic encasement may be more significant on the stone columns subjected to lateral loads. The stone columns may be subjected to significant lateral loads below the toe of high embankments or during large shear movements within the ground. Murugesan and Rajagopal [51] have investigated the performance of ordinary stone columns and geosynthetic encased stone columns subjected to shear loading in a long narrow test tank. They have reported that the ordinary stone columns have undergone early shear failure while the geosynthetic encased stone columns could withstand much higher lateral loading.

Mohapatra et al. [65] and Mohapatra and Rajagopal [66] have reported the results from large-scale direct shear tests

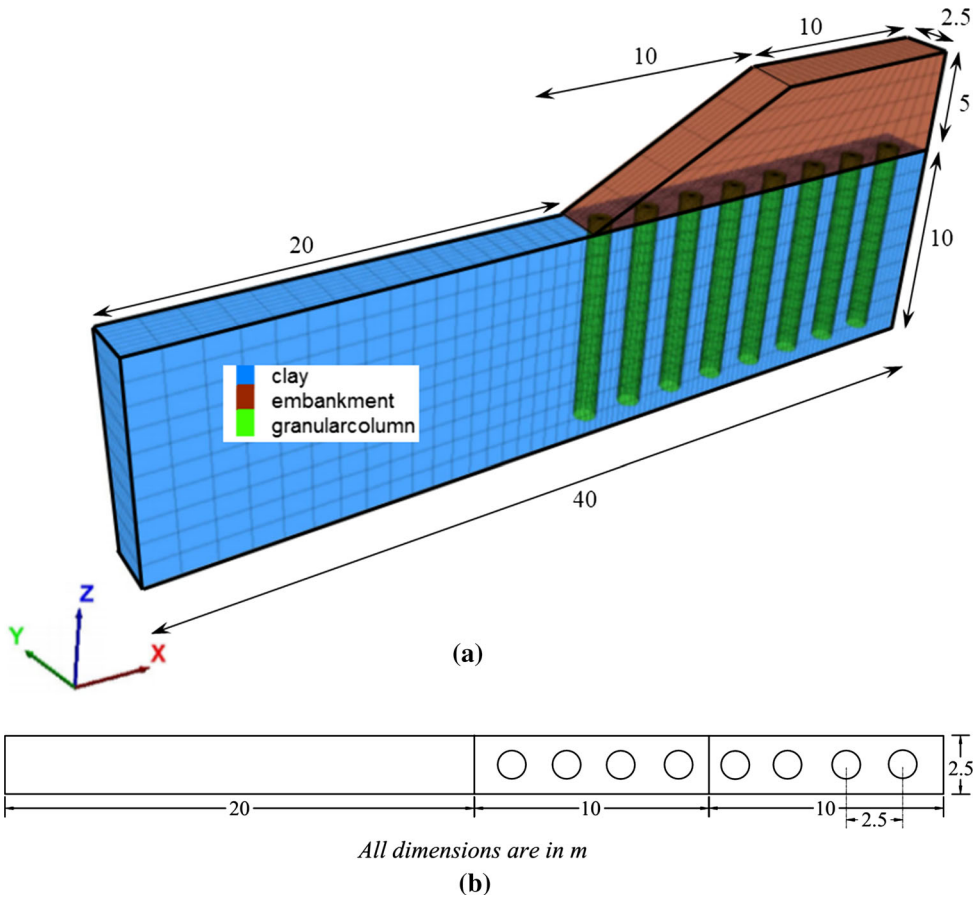

Fig. 55 Numerical model of embankment supported on granular column treated soil. **a** Three dimensional view, **b** plan view [67]

on geosynthetic encased granular columns arranged in different group patterns. They have observed that the shear strength with geosynthetic encased granular columns is higher than that with ordinary granular columns. The soil samples reinforced with ordinary granular columns have reached a peak stress and after that their strength remained constant as the granular columns have undergone clean rupture failure under the shear deformations. On the other hand, the soil samples reinforced with encased granular columns have exhibited strain hardening type behaviour with increasing shear strength with further shear straining.

The influence of geosynthetic encasement on the strength of granular columns was investigated by Mohapatra and Rajagopal [66] and Mohapatra [67] through slope stability analysis of embankments resting on soft clay foundation soil. Numerical analyses were performed using 3-dimensional models using the FLAC3d program, Fig. 55. The embankment was assumed to be constructed on a granular column treated foundation soil having low shear strength of 10 kPa. The analyses were performed with and without geosynthetic encasement. In the case of ordinary stone columns, the rupture planes passed through the foundation soil indicating deep seated failure, Fig. 56. The factor of safety was very low until the area replacement was increased to more than 20%. The analysis with encased granular columns showed higher factors of safety. As expected, the factor of safety was found to depend on the modulus of the geosynthetic encasement, Table 6. As the encasement modulus was increased, the nature of failure changed from deep seated to toe failure indicating that the foundation soil is too strong for the given loading conditions.

The vertical load capacity of the encased granular columns can be estimated by combining the conventional equations with the additional encasement provided by the geosynthetic encasement. Murugesan [64] and Murugesan and Rajagopal [52] have proposed a simple method to incorporate the effect of encasement on the strength of the granular columns. The results from different laboratory tests and finite element based numerical analyses are reported in the form of a design chart as shown in Fig. 57 to estimate the tensile strength required of the encasement material. The new German design code EBGEO [68] has given a detailed procedure for estimating the load capacity and settlement reduction due to the installation of encased stone columns.

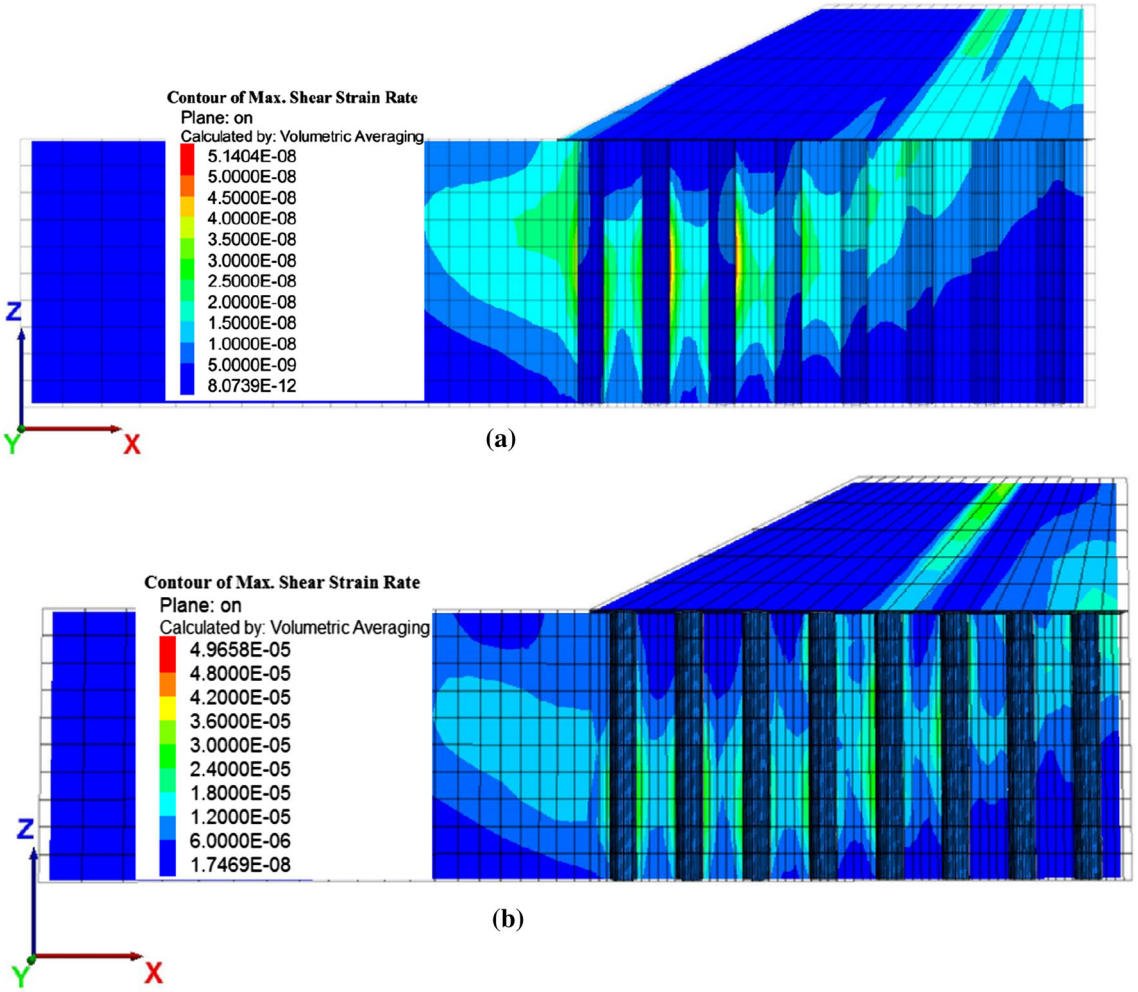

Fig. 56 Shear strain contours with different types of granular columns [67]. **a** Ordinary granular columns, **b** encased granular columns

Table 6 Factor of safety for different analysis cases

A_s (%)	FS		
	OSC	ESC	
		J = 500 kN/m	J = 2500 kN/m
8.04	0.83	0.98	1.29
12.56	0.93	1.03	1.29
18.09	0.97	1.14	1.30
24.62	1.02	1.24	1.30

Geosynthetic Load Transfer Platforms (GRPES)

The geosynthetic load transfer platforms are similar to the pile raft foundations. Instead of the rigid raft, horizontal layers of geosynthetic reinforcement layers are provided. This foundation system is a flexible system in which the deformations are promoted to some extent in order for the soil arching to develop and transferring higher loads into the column elements. The principle of this method is schematically explained in Fig. 58.

The diameter, length and centre to centre (c/c) spacing of piles and the basal reinforcement layers are designed to minimize the total and differential settlements within the allowable limits. Due to the arching mechanism within the embankment, higher loads are transferred to the geosynthetic reinforcement layers and the piles. The GRPES support systems are reported to be economical for both the initial construction and their long term maintenance [69].

Load transfer in the geosynthetic reinforced piled embankments is mainly due to two mechanisms. Firstly soil arching develops as the embankment fill mass between piles has a tendency to move downward due to the presence of soft foundation soil. This movement is partially restrained by shear resistance from the fill above the piles. The shear resistance reduces the pressure acting on the reinforcement but increases the load applied onto the pile caps (Fig. 59). This load transfer mechanism is the classical soil arching [1].

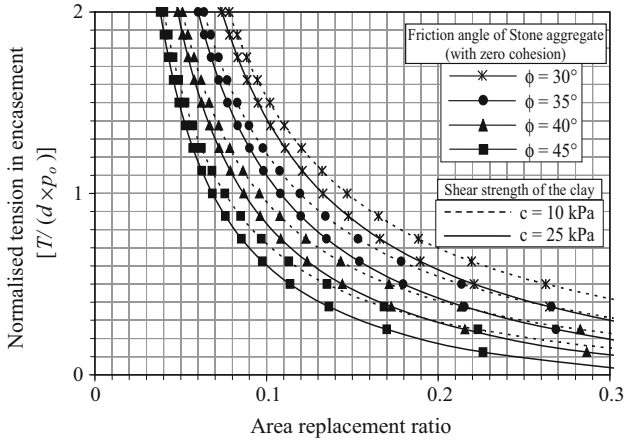

Fig. 57 Design chart for selection of geosynthetic for encased granular columns [64]

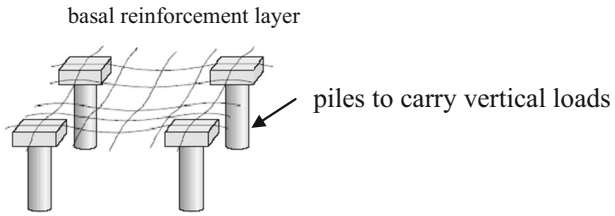

Fig. 58 Schematic of the geosynthetic load transfer platform

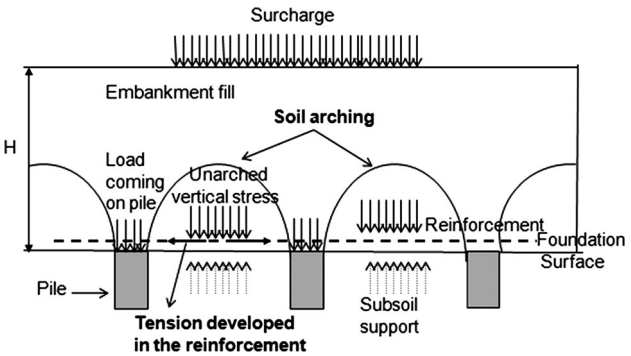

Fig. 59 Mechanism in geosynthetic load transfer platforms [73]

The arches span the soft soil and the applied load is transferred onto the piles and then the firm bearing stratum [70]. Secondly the some part of the vertical stress between the columns is assumed to be carried by the geosynthetic reinforcement. This load applied normal to the surface of the reinforcement creates tension in the membrane, creating the membrane effect [71]. Then this load is transferred to the columns through the vertical component of the tensile forces in the membrane [72]. Figure 59 shows the direction of tensile force developed in the reinforcement.

The British code [17] has given a method of design of the load transfer platforms with end bearing piles and floating piles. These solutions are given for immediate undrained response. However, [74, 75] have reported that the consolidation of soils plays an important role in the manner of load transfer. They have performed full-scale 3-dimensional finite element analyses to investigate various aspects of these load transfer platforms such as number of reinforcement layers, floating piles with different lengths, end bearing piles and consolidation settlements. The 3-dimensional finite element model for these numerical analyses is shown in Fig. 60.

The magnitudes of loads transferred to the piles for different cases are shown in Table 7. The 36 m long pile is an end bearing pile and the others are floating piles. The force transferred into the floating piles is found to be a function of the length of the piles and degree of consolidation. The gradual increase of loading in piles is shown in Fig. 61. The load transfer into the piles and the intervening clay soil is illustrated through the stress vectors in Fig. 62 for the case of end bearing pile. The direction of stress vectors are more prominently pointed into the pile some time after the consolidation indicating the load transfer. From the direction of stress vectors in Fig. 62, it could be understood that the pressure transferred into the foundation soil is progressively reduced with consolidation.

Based on the estimated loads for different cases of floating piles and the end bearing piles, the following modified equations are proposed for the arching coefficient (C_c). As the load transferred to the floating piles are found to be dependent on their length and the location of the neutral plane, these two lengths are incorporated in the equation for arching coefficient of floating piles.

End of construction

$$C_c = 1.8\left(1.95\frac{H}{a} - 0.18\right) \text{ for end bearing piles}$$

$$C_c = 2.2\left(1.5\frac{H}{a} - 0.07\right) = 5.8\left(\frac{\bar{x}}{l_{crit}}\right)\left(1.5\frac{H}{a} - 0.07\right) \text{ for floating piles} \quad (13)$$

End of consolidation

$$C_c = 2.5\left(1.95\frac{H}{a} - 0.18\right) \text{ for end bearing piles}$$

$$C_c = 2.8\left(1.5\frac{H}{a} - 0.07\right) = 7.4\left(\frac{\bar{x}}{l_{crit}}\right)\left(1.5\frac{H}{a} - 0.07\right) \text{ for floating piles} \quad (14)$$

where $\bar{x}$ is the depth of neutral plane at the end of consolidation, H is the height of embankment, a is the pile diameter and ℓ_{crit} is the critical length of the floating pile.

At the moment, the design of geosynthetic reinforced load transfer platform is based on empirical and some semi-analytical methods. Recently, there is one design document prepared by van Eekelen and Brugman [76] for

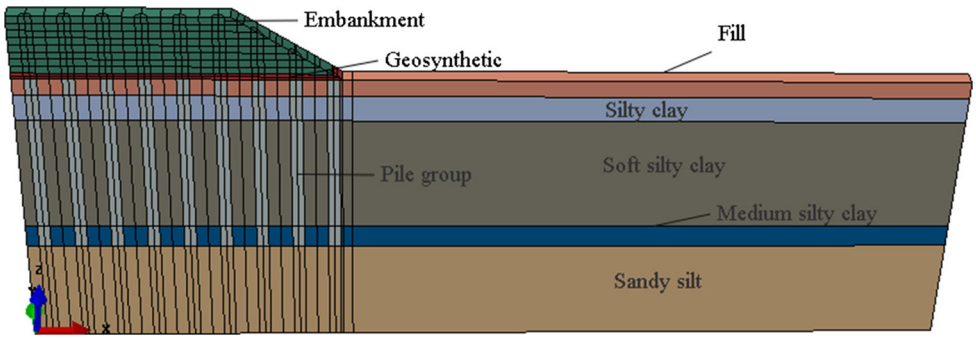

Fig. 60 Finite element model for the analysis of geosynthetic reinforced load transfer platform [74]

Table 7 Loads transferred into piles at different stages

Pile length, ℓ (m)	End of construction	End of consolidation	
	Maximum axial force developed (kN)	Maximum axial force developed (kN)	% increase in axial force compared to 15 m long pile
15 m	194.4	316	
18 m	195.5	341.3	8.0
22 m	197.8	370.4	17.2
36 m	543	651.1	106.0

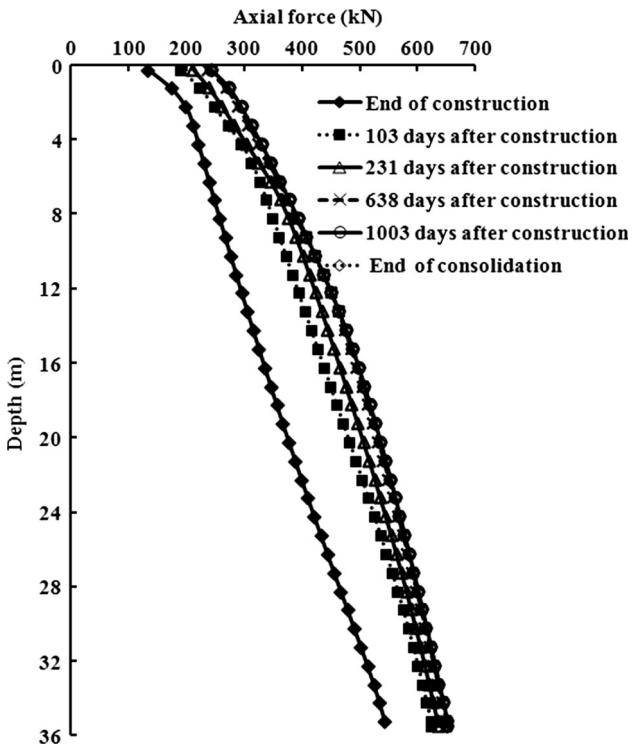

Fig. 61 Load transferred into the end bearing pile at different times [74]

these structures. The validity of the above proposed equations is being verified currently against the data from scale model tests being performed in the centrifuge facility at IIT Bombay.

Vacuum Induced Consolidation of Soft Soils

The original theory for using the atmospheric pressure to induce consolidation of clay soils in place of surcharge loading was developed more than 60 years back by Kjellman [77]. The introduction of geosynthetic products, particularly the geomembranes and PVDs has made it practicable to implement the vacuum technology for soil consolidation. There are several fundamental differences in the manner of consolidation induced by vacuum and the surcharge method as highlighted in Table 8.

Because of the above reasons, the vacuum method is more efficient compared to the surcharge method. There are basically two methods for applying the vacuum method of consolidation. The membrane covered system involves in isolating the entire treatment area by covering with a thick geomembrane and deep all round trenches filled with bentonite slurry. The membrane less method is much simpler wherein the vacuum is applied at some depth below the relatively impermeable top soil.

Ganesh et al. [78] and Ganesh [79] have investigated the comparison between the vacuum and surcharge induced consolidation of soft clay soils through tests on a column of soft clay soil consolidation by both methods. The time rate of settlement, moisture content at different depths and the pressure–settlement responses were evaluated after consolidation by both methods. Figure 63 shows the set up for the vacuum consolidation of clay soil.

A comparison between the time rates of consolidation obtained in both methods is shown in Fig. 64 at a

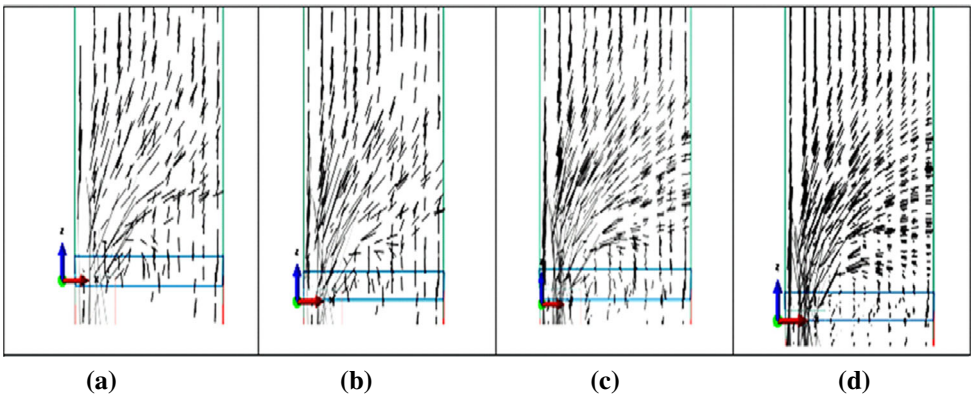

Fig. 62 Development of arching in the case of end bearing piles [74]. **a** During construction (H = 8.5 m), **b** during construction (H = 10 m), **c** 30 days after construction, **d** 100 days after construction

Table 8 Differences between the vacuum and surcharge induced consolidation

Sl. No.	Item	Surcharge method	Vacuum method
1	Nature of effective stresses	Anisotropic stress increments	Isotropic stress increments
2	Total stresses	Increase in total stresses	Remains the same
3	Nature of driving the consolidation	Surcharge loading applied to drive the consolidation	Atmospheric pressure used to drive the consolidation
4	Time rate of increase in effective stresses	Gradually increases with the progress in consolidation	Almost instantaneous as there are no increase in total stresses
5	Variation of effective stresses with depth	Reduces with depth due to stress dispersion	Stress increment remains constant with depth except for losses in vacuum pressure
6	Shear stresses	Shear stresses are generated due to anisotropic increase of vertical and horizontal stresses under surcharge	Zero as the effective stress increment is isotropic
7	Internal shear deformations during consolidation	Likely due to increase in shear stresses	Not likely as the shear stress increments are zero
8	Nature of ground movements	Outward movements due to the shear stress generation under surcharge loading	Inward movements due to isotropic compression—cracks may appear on the ground surface around the treated zone

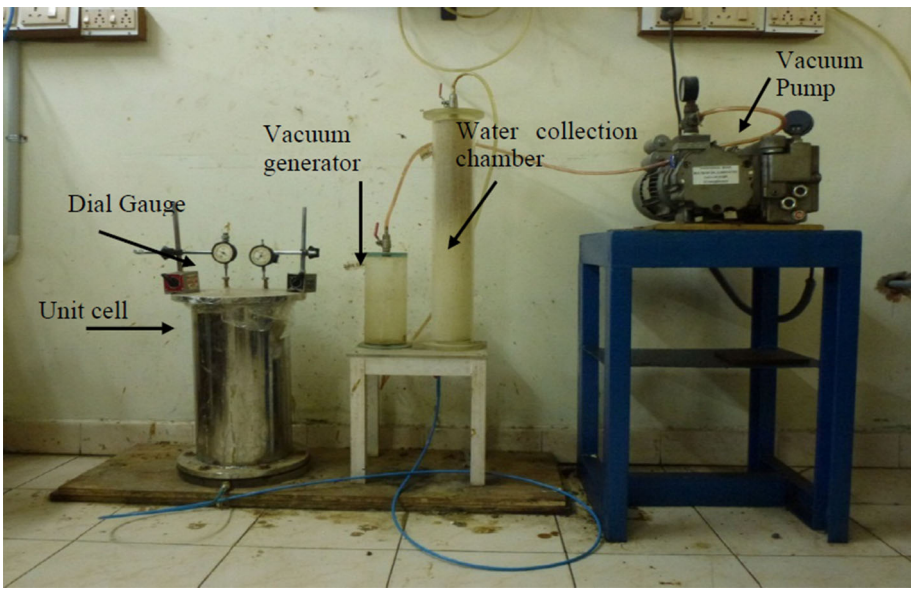

Fig. 63 Set up for vacuum consolidation of clay soil [79]

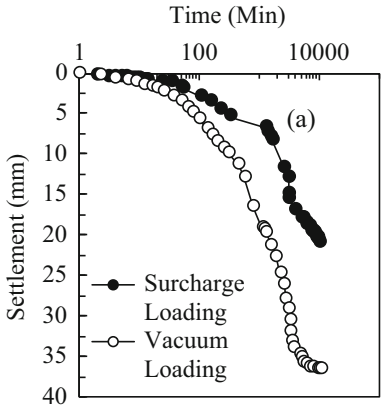

Fig. 64 Comparison between vacuum and surcharge consolidations [79]

Table 9 Comparison of water contents after consolidation by surcharge and vacuum

Location	Water content (%) under 65 kPa pressures	
	Surcharge	Vacuum
Top	41.7	39.3
Middle	45.1	39.4
Bottom	45.5	38.4

consolidation pressure of 65 kPa. The vacuum induced consolidation is quicker and is able to achieve much higher consolidation settlement as clearly evident from the figure. It is clear that vacuum method is faster than the surcharge method. Comparison of the water contents at three different depths at the end of consolidation under 65 kPa pressure is shown in Table 9. The initial water content of the soil was 48%. The water content with vacuum consolidation is more or less constant with depth indicating that the influence of the pressure is uniform with depth. On the other hand, the surcharge consolidation gave lesser water content at top and higher water contents at higher depths. This is due to the gradual reduction of surcharge effects with depth.

The vacuum consolidation method was demonstrated through a field test in Kakinada as reported by Ganesh et al. [80]. They have used both vacuum and surcharge methods of consolidation on an experimental basis within the Kakinada port trust grounds. The procedure used for vacuum application was the membrane less method wherein the vacuum pipe was connected to the PVD at a depth of 4 m. The vacuum pressure was applied to the clay soil within the depths of 4–15 m below the ground level through PVDs. The schematic for both methods of consolidation is shown in Fig. 65. The test had to be terminated after 3 weeks due to a cyclonic disturbance. The ground settlements, pore water pressures were monitored during the consolidation. The strength of the top 3–4 m of soil was assessed using light cone penetrometer test (LCPT).

The rate of vacuum induced settlements was found to be marginally faster than those under surcharge consolidation. As the area of treatment was very small at 10 × 10 m plan

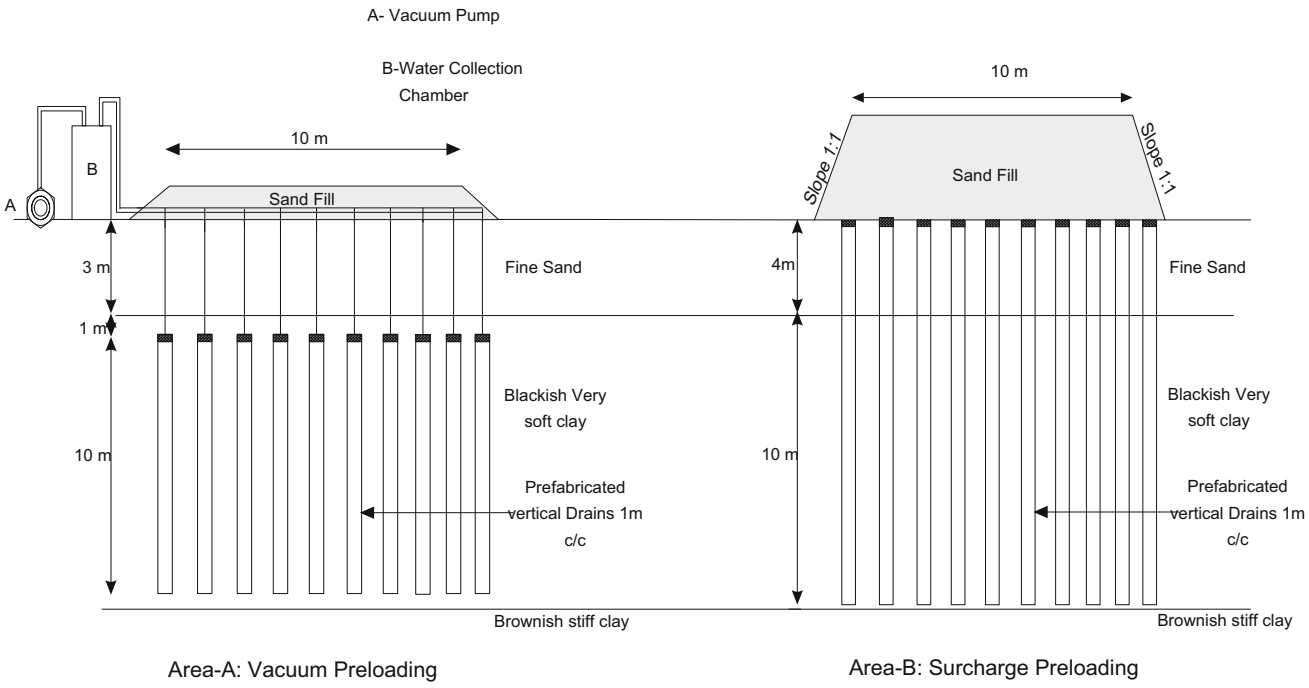

Fig. 65 Schematic of field trials of vacuum and surcharge induced consolidation [80]

area, the differences were not significant. The penetration resistance of the soil was periodically monitored. The penetration resistance was found to increase significantly due to the consolidation. The experience gained from this project include the method of connection of vacuum pipe with PVD, mechanism of vacuum application in a field-scale test and monitoring the settlements during the consolidation process.

Environmental Sustainability Using Geosynthetics

The issue of environmental sustainability in construction projects needs to be addressed due to the fast depleting natural resources. At most construction sites, natural materials like good quality sands and aggregate are not available at short distances. Their transportation from large distances entails huge expenditure and consumption of fuel leading to excessive carbon foot print to the project. The use of geosynthetics leads to reduced consumption of natural materials due to steep soil slopes, reduced quantities of aggregate thicknesses, larger spacing of stone columns, etc. For example, it is possible to completely replace the drainage blankets made of natural aggregates with geosynthetic drainage products as shown in Fig. 66.

The data collected from a highway construction site near Chennai was analyzed in detail based on the design cross-sections with and without geosynthetics, distance to the quarry site, typical costs of natural materials and the fuel consumed for transporting the materials. The results of these analyses are presented in Fig. 67 that clearly shows that the use of geosynthetics in highway projects leads to saving of cost and time in addition to reducing the carbon footprint. The construction times with geosynthetics are reduced due to lesser times involved in transporting the quarry materials, lesser times for spreading and compacting them. For the same reason, the carbon footprint is also reduced. In all these calculations, the unreinforced section is taken as 100% against which the other quantities are compared [81].

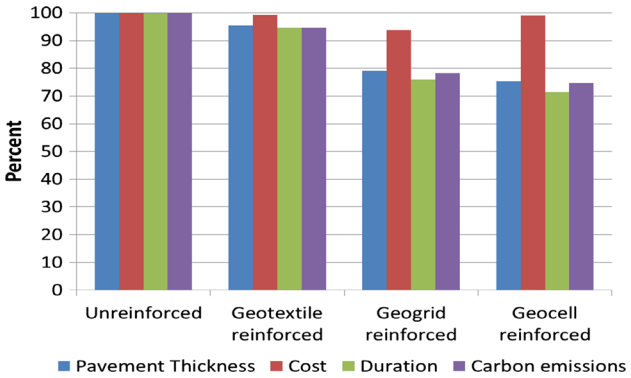

Fig. 67 Comparison for a highway construction with different geosynthetic materials [81]

Another application of geosynthetics where local beach sand can be used along with geosynthetics also is an environmentally friendly compared to the use of boulders, stones or reinforced concrete elements. The beach sand can be used along with geotubes, geobags filled in gabion boxes, etc. as illustrated in Fig. 68.

The geocells also offer lot of potential for use of locally available marginal soils for construction of retaining walls, highway pavements, erosion control structures, etc. Through field and laboratory studies [82] have demonstrated the benefit of using different types of geosynthetic in road pavement structures. Systematic full-scale research works are required before their usage can be incorporated in codal provisions for wide spread usage of these techniques in highway applications.

Conclusions

This lecture has introduced the geosynthetic materials, their background and their strength aspects. Their application to different infrastructure projects was discussed. These products have received wide acceptance by the geotechnical engineers all over the world. The details of some of these constructions and results from some

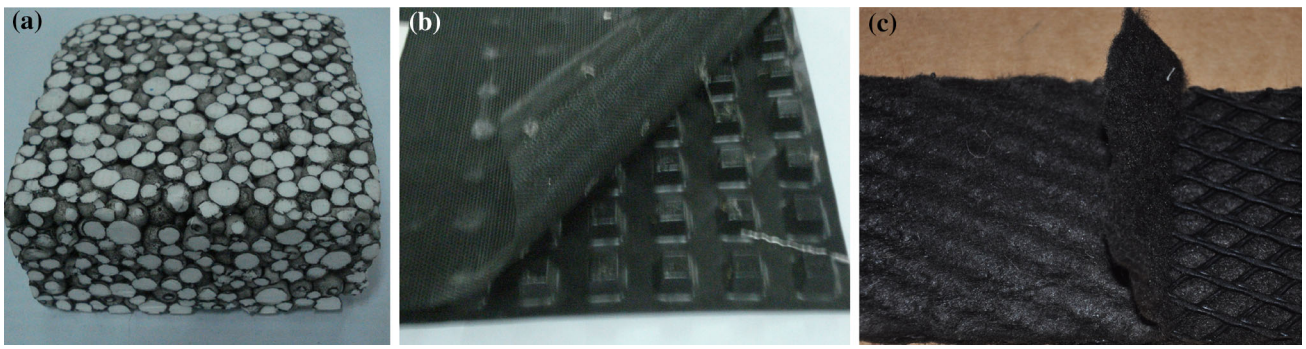

Fig. 66 Some geosynthetic drainage products. **a** Drain with EPS beads, **b** sheet drain, **c** geonet and geotextile

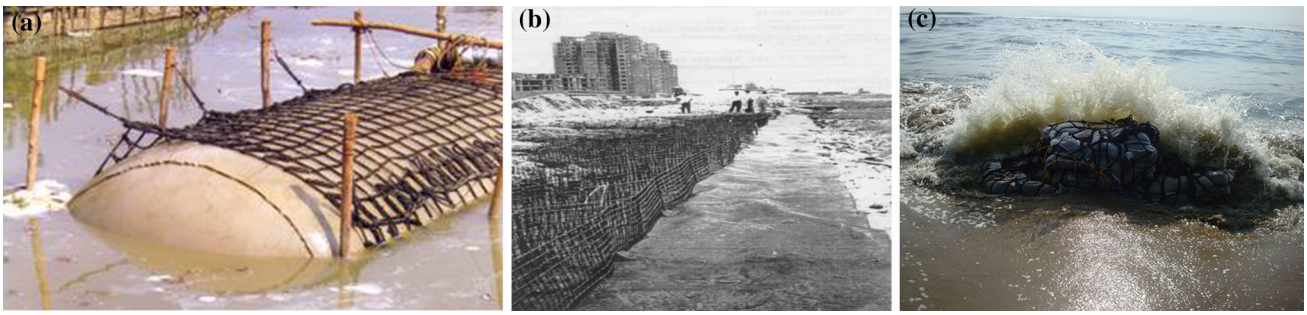

Fig. 68 Different geosynthetic techniques for coastal erosion protection

theoretical and experimental investigations are presented. The limited strength of the soil can be easily overcome using the sandwich technique, geocell confinement, etc. as described. Adequate cross-references are given for the readers to get more details on the works reported in this lecture.

Acknowledgements Firstly, I would like to thank the Indian Geotechnical Society for giving me this prestigious opportunity to address the august gathering of geotechnical engineers from India and abroad. My sincere thanks are due to IIT Madras for providing excellent ambience and nurturing every step taken in search of answers to different questions in geotechnical engineering. My special thanks to all my faculty colleagues in geotechnical engineering at IIT Madras for their enthusiastic discussions, research collaborations and helpful suggestions. Especially, I would like to place on record my appreciation to Prof. N.R. Krishnaswamy who provided full support in initiating my teaching and research career at IIT Madras. Most of all, my thanks are to all my former doctoral students, Unnikrishnan, Madhavi Latha, Jeyalakshmi, Purnanandam, Sujit Kumar Dash, Sajna, Murugesan, Karthigeyan, Ranga Swamy, Anjana Bhasi, Ganesh, Sridhar and Sunil Ranjan Mohapatra. Thanks are also due to the current doctoral students Murthy, Nithin, Muneeb, Reshma, Chaitanya, Jayapal, Dinesh, Shyamala, Gupta, Kiran and Prabhavathy. Each of them was unique who brought new ideas and fresh energy with each one of them. That made the teaching and research work at IIT Madras exciting and invigorating. The research work reported here could not have been carried out without the financial support from several public and private sponsoring agencies including Department of Science and Technology, Ministry of Human Resource Development, Netlon India Ltd, Garware Wall Ropes Ltd, Techfab (India), Strata Geosystems (India) Ltd, Maccaferri Environmental Solutions Pvt. Ltd India, PRS Mediterranean Ltd. Thanks are due to my family members for their patience, understanding and support to my academic pursuits. Finally, thanks are due to the Almighty Avatar Meher Baba.

References

1. Terzaghi K (1943) Theoretical soil mechanics. Wiley, New York
2. Koerner RM (2012) Designing with geosynthetics, vol 1&2, 6th edn. Xlibris Corporation, Bloomington
3. Giroud JP (1986) From geotextiles to geosynthetics: a revolution in geotechnical engineering. In: Proceedings of 3rd international conference on geotextiles, Vienna, Austria, pp 1–18
4. Rao GV, Saxena KR (1989) Use of geosynthetics in India experiences and potential. Central Board of Irrigation and Power, New Delhi
5. Rao GV (1996) Geosynthetics in the Indian environment, IGS lecture 1995. Indian Geotech J 26(1):1–94
6. Rao GV (2016) Indian perspective—achievements and projections. In: Heritage lecture delivered at 6th Asian regional conference on geosynthetics, November 8–11, New Delhi, pp HL3–HL36
7. Rao GV, Venkatraman M, Knajlia VK, Gupta AC (2016) History of geosythetis in India—case studies, Publication No. 332. Central Board of Irrigation and Power, New Delhi
8. Maher M, Gray D (1990) Static response of sands reinforced with randomly distributed fibers. ASCE J Geotech Eng 116(11):1661–1677
9. Bathurst RJ, Rajagopal K (1993) Large-scale triaxial compression testing of geocell-reinforced granular soils. ASTM Geotechn Test J 16(3):296–303
10. Rajagopal K, Krishnaswamy NR, Latha GM (1999) Behaviour of sand confined with single and multiple geocells. J Geotext Geomembr 17(3):171–184
11. Meher S (2012) Summer internship report titled strength properties of reinforced soil. Department of Civil Engineering, IIT Madras, Chennai
12. Chandrasekaran B, Broms BB, Wong KS (1989) Strength of fabric reinforced sand under axisymmetric loading. Geotext Geomembr 8:293–310
13. Schlosser F, Long NT (1973) Etude du comportement du materiau terre armee. Annales de l'Inst., Techq. du Batiment et des Trav. Publ. Suppl. No. 304, Ser. Mater. No. 45
14. Yang Z (1972) Strength and deformation characteristics of reinforced sand. Ph.D. thesis, University of California, Los Angeles, USA
15. Hausmann MR (1976) Engineering principles of ground modification. McGraw-Hill Publishing Co, New York
16. Jewell RJ (1996) Soil reinforcement with geotextiles, Special Publication No. 123 of CIRIA. Thomas Telford, London, UK
17. BS8006 (2010) Code of practice for strengthened/reinforced soils and other fills. British Standards Institution, London
18. Federal Highway Administration (2010) Design and construction of mechanically stabilized earth walls and reinforced soil slopes, vol I & II, Publication No. FHWA-NHI-10-024 & FHWA-NHI-10-025. US Department of Transport, Washington, DC, USA
19. Sreedharan A, Murthy SBR, Revanasiddappa K (1991) Technique for using fine-grained soil in reinforced earth. J Geotech Eng Div ASCE 117(8):1174–1189
20. Unnikrishnan N (1998) Investigations on reinforced soil embankments subjected to monotonic and cyclic loading. Thesis submitted in partial fulfilment of the requirements for Ph.D. degree, Indian Institute of Technology Madras, Chennai
21. Unnikrishnan N, Rajagopal K, Krishnaswamy NR (2002) Triaxial behaviour of reinforced clay under static and cyclic loading. Indian Geotech J 32(3):216–234

22. Milligan GWE, Earl RF, Bush DI (1990) Observation of photoelastic pullout tests on geotextiles and grids. In: Proceedings of 4th international conference on geotextiles geomembranes and related products, Hague, Netherlands, vol 2, pp 747–751
23. Rajagopal K (1995) User's manual for the finite element program GEOFEM2. Department of Civil Engineering, Indian Institute of Technology Madras, Chennai
24. Wathugala GW, Desai CS (1993) Constitutive model for cyclic behavior of clays I: theory. J Geotech Eng ASCE 119:714–729
25. Henkel DJ, Gilbert GC (1952) The effect of rubber membranes on the measured triaxial compressive strength of clays. Geotechnique 3:20–29
26. Latha GM (2000) Investigations on the Behaviour of geocell supported embankments. Thesis submitted in partial fulfilment of the requirements for Ph.D. degree, Indian Institute of Technology Madras, Chennai
27. Latha GM, Dash SK, Rajagopal K, Krishnaswamy NR (2001) Finite element analysis of strip footing supported on geocell reinforced sand beds. Indian Geotechn J 31(4):454–478
28. Latha GM, Dash SK, Rajagopal K (2008) Equivalent continuum simulations of geocell reinforced sand beds supporting strip footings. Geotechn Geol Eng 26:387–398
29. Dash SK, Krishnaswamy NR, Rajagopal K (2001) Bearing capacity of strip footings supported on geocell-reinforced sand. J Geotext Geomembr 19:235–256
30. Latha GM, Rajagopal K, Krishnaswamy NR (2006) Experimental and theoretical investigations on geocell supported embankments. ASCE Int J Geomech 6(1):30–35
31. Madhavi Latha G, Rajagopal K (2007) Parametric finite element analysis of geocell supported embankments. Can Geotechn J 44:917–927
32. Rajagopal K, Madhav MR, Raju PT, Sreedhar V, Loke KH (2010) Construction and monitoring of a 22.5 m high geosynthetic segmental retaining wall in India, Paper No. 78. In: Proceedings of 6th international conference on geosynthetics, Guaruja, Brazil, May 23–27, 2010
33. Raju PT (2012) Tiered geosynthetic reinforced soil retaining walls for widening of ghat road at vijayawada, advances in geosynthetics. Saimaster Geoenvironmental Services Pvt. Ltd, Hyderabad, pp 157–165
34. NCMA (2009) Design manual for segmental retaining walls, 3rd edn. National Concrete Masonry Association, Virginia
35. ASTMD 6638-2001. Standard test method for determining connection strength between geosynthetic reinforcement and segmental concrete units (modular concrete blocks). American Society for Testing and Materials, West Conshohocken, pp 19428–2958
36. Greeman A (2011) Indian slope tricks. New Civil Engineer, UK, pp 1–4
37. Gharpure AD, Kumar S, Scotto M (2012) Composite soil reinforcement system for retention of very high and steep fills—a case study. In: Proceedings of 5th European geosynthetics congress, Valencia, vol 5, pp 346–352
38. Zhong Z, Xu F, Rimoldi P, Scotto M, Meenu PS (2016) Application of composite reinforced soil structure in airport high walls and slopes. In: Proceedings of 6th Asian regional conference on geosynthetics, New Delhi, 8–11 November, pp 375–381
39. Sivakumar Babu GL, Sporer H, Zanzinger H, Gartung E (2001) Assessment of self healing properties of geosynthetic clay liners. Geosynth Int 8(5):461–470
40. Venkatraman M, Sreenivas K (2004) Hazardous waste landfills—Indian case studies, geosynthetics—new horizons. In: Rao GV, Banerjee PK, Sahu JT, Ramana GV (eds) Geosynthetics - New Horizons. M/s Asian Books Pvt. Ltd, New Delhi, pp 243–250
41. Dash R, Rajagopal K, Arnepalli DN (2016) Design and Development of increased storage capacity of a lined pond at Hindustan Zinc Ltd. In: Proceedings of 6th Asian regional conference on geosynthetics, November 8–11, 2016, New Delhi, pp 591–598
42. Barksdale RD, Bachus RC (1983) Design and construction of stone columns. Report No. FHWA/RD-83/026, Federal Highway Administration Office of Engineering and Highway Operations Research and Development Washington, DC
43. Greenwood DA (1970) Mechanical improvement of soils below ground surface. In: Ground engineering proceedings of the conference by the institution of civil engineers, London, pp 11–22
44. Hughes JMO, Withers NJ, Greenwood DA (1975) A field trial of the reinforcing effect of a stone column in soil. Geotechnique 25(1):31–44
45. IS 15284-Part 1 (2003) Indian standard—design and construction for ground improvement—guidelines. Part—1. Stone Columns, New Delhi
46. Chummar AV (2000) Ground improvement using stone columns: problems encountered. In: An international conference on geotechnical and geological engineering, GeoEng2000, Melbourne, Australia
47. Thorburn S (1975) Building structures supported by stabilized ground. Geotechnique 25(1):83–94
48. McKenna JM, Eyre WA, Wolstenholme DR (1975) Performance of an embankment supported by stone columns in soft ground. Geotechnique 25(1):51–59
49. Murugesan S, Rajagopal K (2006) Geosynthetic encased stone columns: numerical evaluation. J Geotext Geomembr 24:349–358
50. Murugesan S, Rajagopal K (2007) Model tests on geosynthetic-encased stone columns. Geosynth Int 14(6):346–354
51. Murugesan S, Rajagopal K (2008) Shear load tests on granular columns with and without geosynthetic encasement. Geotech Test J 32(1):35–44
52. Murugesan S, Rajagopal K (2010) Studies on the behavior of single and group of geosynthetic encased granular columns. J Geotechn Geoenviron Eng 136(1):129–139
53. Yoo C, Kim SB (2009) Numerical modeling of geosynthetic-encased granular column-reinforced ground. Geosynth Int 16(3):116–126
54. Gniel J, Bouazza A (2010) Construction of geogrid encased granular columns: a new proposal based on laboratory testing. Geotext Geomembr 28(1):108–118
55. Khabbazian M, Kaliakin VN, Meehan CL (2011) Performance of quasilinear elastic constitutive models in simulation of geosynthetic encased columns. Comput Geotech 38:998–1007
56. Lo SR, Zhang R, Mak J (2010) Geosynthetic-encased stone columns in soft clay: a numerical study. Geotext Geomembr 28(3):292–302
57. Malarvizhi SN, Ilamparuthi K (2004) Load versus settlement of claybed stabilized with stone and reinforced stone columns. In: Asian regional conference on geosynthetics, GeoAsia—2004, pp 322–329
58. Dash SK, Bora MC (2013) Influence of geosynthetic encasement on the performance of stone columns floating in soft clay. Can Geotech J 50(7):754–765
59. Elsawy MBD (2013) Behaviour of soft ground improved by conventional and geogrid-encased stone columns, based on FEM study. Geosynth Int 20(4):276–285
60. Chen J-F, Li L-Y, Xue J-F, Feng S-Z (2015) Failure mechanism of geosynthetic-encased stone columns in soft soils under embankment. Geotext Geomembr 43(5):424–431
61. Raithel M, Kempfert HG (2001) Practical aspects of the design of deep geotextile coated sand columns for the foundation of a dike on very soft soils. In: Proceedings of the international conference on landmarks in earth reinforcement, Switzerland, pp 545–548
62. Raithel M, Kempfert HG, Kirchner A (2002) Geotextile-encased columns (GEC) for foundation of a dike on very soft soils. In: Seventh international conference on geosynthetics, Nice, France, pp 1025–1028

63. Raithel M, Kirchner A, Schade C, Leusink E (2005) Foundation of constructions on very soft soils with geotextile encased columns—state of the art. Geotech Spec Publ 130–142:1867–1877
64. Murugesan S (2008) Geosynthetic encased stone columns as ground reinforcement of soft soils. Thesis submitted in partial fulfilment of the requirements for Ph.D. degree, Indian Institute of Technology Madras, Chennai
65. Mohapatra SR, Rajagopal K, Sharma JS (2016) Large direct shear load tests on geosynthetic encased granular columns. Geotext Geomembr 44(3):396–405
66. Mohapatra SR, Rajagopal K (2016) Analysis of failure of geosynthetic encased stone column supported embankments. In: Proceedings of 3rd Pan-American conference on geosynthetics, April, Miami Beach, USA
67. Mohapatra SR (2016) Analysis of the behaviour of ordinary and geosynthetic encased granular columns subjected to shear loading. Thesis submitted in partial fulfilment of the requirements for Ph.D. degree, Indian Institute of Technology Madras, Chennai
68. EBGEO (2011) Recommendations for design and analysis of earth structures using geosynthetic reinforcements, German geotechnical society. Ernst & Sohn, Berlin
69. Alexiew D, Gartung E (1999) Geogrid reinforced railway embankments on piles: performance monitoring 1994–1998. In: Proceedings of the 1st South American symposium on geosynthetics/3rd Brazilian symposium on geosynthetics, Rio de Janerio, pp 403–411
70. Kempfert HG, Gobel C, Alexiew D, Heitz C (2004) German recommendations for reinforced embankments on pile-similar elements. In: Proceedings of the EuroGeo3, Munich DGGT, pp 279–284
71. Zhan C, Yin JH (2001) Elastic analysis of soil-geosynthetic interaction. Geosynth Int 8:27–48
72. Han J, Gabr M (2002) Numerical analysis of geosynthetic-reinforced and pile-supported earth platforms over soft soil. J Geotechn Geoenviron Eng 128(1):44–53
73. Lawson CR (2012) Role of modelling in the development of design methods for basal reinforced piled embankments. In: Proceedings of EuroFuge 2012, Delft, The Netherland
74. Bhasi A (2013) Performance evaluation of geosynthetic reinforced embankments supported on piles. Thesis submitted in partial fulfilment of the requirements for Ph.D. degree, Indian Institute of Technology Madras, Chennai
75. Bhasi Anjana, Rajagopal K (2014) Geosynthetic-reinforced piled embankments: comparison of numerical and analytical methods. ASCE Int J Geomech. doi:10.1061/(ASCE)GM.1943-5622.0000414
76. Van Eekelen SJM, Brugman MHA (2016) Design guideline basal reinforced piled embankments. CRC Press/Balkema, Delft
77. Kjellman W (1952) Consolidation of clay soil by means of atmospheric pressure. In: Proceedings of conference on soil stabilization MIT, Cambridge, pp 258–263
78. Kumar SG, Robinson RG, Rajagopal K (2014) Improvement of soft clays by combined vacuum consolidation and geosynthetic encased stone column. Indian Geotech J 44(1):59–67
79. Kumar SG (2014) Treatment of soft clay deposite by combined encased stone column and vacuum consolidation. Thesis submitted in partial fulfilment of the requirements for the award of Ph.D. Degree, Indian Institute of Technology Madras, Chennai
80. Kumar SG, Sridhar G, Radhakrishnan R, Robinson RG, Rajagopal K (2015) A case study of vacuum consolidation of soft clay deposit. Indian Geotechn J 45(1):51–61
81. Vandana M (2013) Influence of geosynthetic reinforcement on carbon footprint of flexible pavements. M.Tech. Thesis, Department of Civil Engineering, IIT Madras, Chennai
82. Rajagopal K, Chandramouli S, Parayil A, Iniyan K (2014) Studies on geosynthetic-reinforced road pavement structures. Int J Geotech Eng 8(3):287–298

Rajagopal Karpurapu Dr Rajagopal has been teaching at IIT Madras since 1993. Prior to that he worked at Carleton University, Ottawa and Royal Military College of Canada, Kingston where he was exposed to different aspects of geotechnical and geosynthetic engineering. He was promoted to professor position in the year 2000 at IIT Madras. He had served as Head of the Department of Civil Engineering at IIT Madras during the period 2008-2011.

At IIT Madras he has worked extensively on the fundamental aspects of the strength ofgeosynthetic reinforced soil and its application to various constructions. The research work includes laboratory tests and finite element-based numerical simulations. He has guided several doctoral and masters students and published extensively in all major international journals. He has received several best paper awards for the papers published. He has taken up several sponsored research projects and consultancy projects in the geosynthetics field. He was given the Life Time Achievement Award by the Central Board of Irrigation and Power in recognition of the services rendered to promote the use of geosynthetic technology in India.

He has been an editorial board member of national and international journals including Journal of Geotextiles and Geomembranes, International Journal of Geosynthetics and Ground Improvement, Indian Geotechnical Journal. He has been a member of the Council of International Geosynthetics Society since 2010. He had also served as Executive Committee member of IGS for two terms. He has travelled extensively to all the six continents of the world to attend international conferences, give lectures or to attend the IGS council meetings.